CZECH
HYDROMETEOROLOGICAL
INSTITUTE

Martin Setvák
CHMI Satellite Department
web: http://www.chmi.cz, http://www.setvak.cz
e-mail: martin.setvak@chmi.cz, setvak@gmail.com

A satellite perspective on interactions between convective storms and the upper atmosphere

Co-authors: Steven Miller, Steven.Miller@colostate.edu
Cooperative Institute for Research in the Atmosphere (CIRA),
Colorado State University, Fort Collins, USA

Xavier Calbet, xcalbeta@aemet.es
Agencia Estatal de Meteorología (AEMET), Madrid, Spain

European Conference on Severe Storms 2019, Krakow, Poland
4 – 8 November 2019

Satellite observations of atmospheric gravity waves, generated by convection

- Observations in visible, near-IR and IR bands (e.g. AVHRR, MODIS, VIIRS, SEVIRI, ABI, …) of various forms of gravity waves at cloud tops of convective storms; features related to gravity wave breaking mechanism, observed at or just above the storm tops – jumping cirrus, above anvil cirrus plumes, „radial cirrus", etc. Various forms of gravity waves in WV absorption bands accompanying storm activity. All of these closely related to / initiated by strong updrafts, manifested by overshooting tops. Typically at levels **8 – 14 km** (at mid-latitudes), near the tropopause and in lowest layers of the stratosphere.

- Atmospheric gravity waves in AIRS (*Atmospheric Infrared Sounder*, Aqua satellite) and IASI (*Infrared Atmospheric Sounding Interferometer*, Metop 1 – 3 satellites) hyperspectral sounding data, in the upper stratosphere (~ **40 km**).

- Concentric gravity waves (CGW) observed in nighttime by the Suomi-NPP and NOAA-20 satellites in their Day/Night Band (DNB) data, high above convective storms, in the airglow (nightglow), at **85 – 100 km** (near the mesopause).

Satellite observations of atmospheric gravity waves, generated by convection

- Observations in visible, near-IR and IR bands (e.g. AVHRR, MODIS, VIIRS, SEVIRI, ABI, …) of various forms of gravity waves at cloud tops of convective storms; features related to gravity wave breaking mechanism, observed at or just above the storm tops – jumping cirrus, above anvil cirrus plumes, „radial cirrus", etc. Various forms of gravity waves in WV absorption bands accompanying storm activity. All of these closely related to / initiated by strong updrafts, manifested by overshooting tops. Typically at levels **8 – 14 km** (at mid-latitudes), near the tropopause and in lowest layers of the stratosphere.

- Atmospheric gravity waves in AIRS (*Atmospheric Infrared Sounder*, Aqua satellite) and IASI (*Infrared Atmospheric Sounding Interferometer*, Metop 1 – 3 satellites) hyperspectral sounding data, in the upper stratosphere (~ **40 km**).

- Concentric gravity waves (CGW) observed in nighttime by the Suomi-NPP and NOAA-20 satellites in their Day/Night Band (DNB) data, high above convective storms, in the airglow (nightglow), at **85 – 100 km** (near the mesopause).

Primary goals of this study

- DNB observations of **concentric gravity waves (CGW)** generated by convective storms in nightglow emissions, **statistics of their occurrence on global scale**,
- basic characteristics of these CGW (horizontal extent, typical wavelengths, …),
- for all cases of CGW detected in DNB, their **manifestation in the AIRS data**
- for selected cases of CGW detected in DNB, their manifestation in IASI data.

Airglow (nightglow) and the VIIRS Day/Night Band

VIIRS Day/Night band range (0.5 – 0.9 µm)

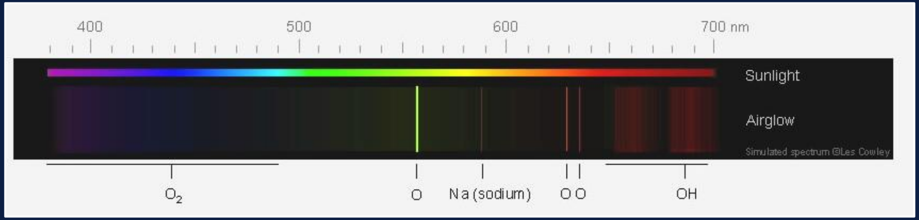

Image source: *http://www.atoptics.co.uk/highsky/airglow2.htm*

Airglow sources – processes related to de-excitation of atoms and molecules, excited by solar ultraviolet radiation during the daytime hours, including chemiluminescence. In contrast to aurora, airglow can be observed globally.

- blue – molecular oxygen, ~ 95 km
- **green** – atoms of oxygen (557.7 nm), 90 – 100 km
- yellow – sodium atoms (589 nm, meteorite origin, or possibly sea salt), ~ 92 km
- red – atoms of oxygen (630, 636.4 nm), 150 – 300 km
- **red and near IR range** – hydroxyl radicals (OH), 85 – 90 km

Given the broadband nature of the VIIRS Day/Night Band, it is not possible to make any inferences about wavelengths of the airglow features observed in this band, and neither about the height of these. All spectral lines between 0.5 and 0.9 µm and airglow layers are superimposed in DNB images. As the emissions at 150-300 km are much weaker compared to those originating between 85 – 100 km, **all nightglow features observed in DNB imagery are located at 85 – 100 km**, near the mesopause.

Example of nocturnal airglow (nightglow) in ground-based photos

Hydroxyl emissions (red and NIR, 85-90 km)

Oxygen 557.7 nm emission (green, 90-100 km)

Yuri Beletsky, 2015/2016, Chile, *www.facebook.com/yuribeletskyphoto*, *www.instagram.com/yuribeletsky/*

SNPP and JPSS (Joint Polar Satellite System) satellites

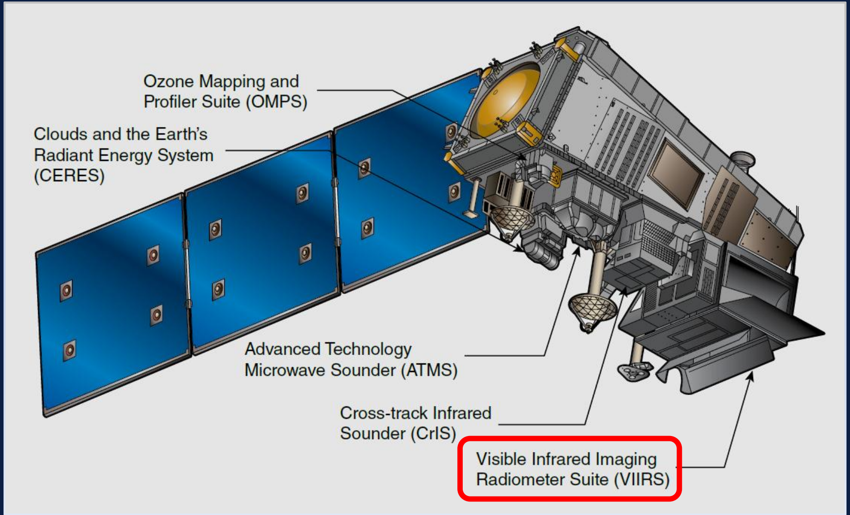

- **Suomi-NPP (SNPP)** – 2011-10-28
- **JPSS-1 / NOAA 20** – 2017-11-18
- JPSS-2 ~ 2022
- JPSS-3 ~ 2026
- JPSS-4 ~ 2031

NOAA-20 on the same orbit as SNPP, half orbit behind, ~ 50 minutes later

- Visible Infrared Imaging Radiometer Suite (VIIRS)
- Advanced Technology Microwave Sounder (ATMS)
- Cross-track Infrared Sounder (CrIS)
- Ozone Mapping and Profiler Suite (OMPS)
- Clouds and the Earth's Radiant Energy System (CERES)

VIIRS (Visible Infrared Imaging Radiometer Suite) – Day/Night Band (DNB)

		Band No.	Wave-length (µm)	Horiz Sample Interval (km Downtrack x Crosstrack)		Driving EDRs	Radi-ance Range	Ltyp or Ttyp	Signal to Noise Ratio (dimensionless) or NEΔT (Kelvins)		
				Nadir	End of Scan				Required	Predicted	Margin
VIS/NIR FPA	Silicon PIN Diodes	M1	0.412	0.742 x 0.259	1.60 x 1.58	Ocean Color Aerosols	Low High	44.9 155	352 316	483 827	37% 162%
VIS/NIR FPA	Silicon PIN Diodes	M2	0.445	0.742 x 0.259	1.60 x 1.58	Ocean Color Aerosols	Low High	40 146	380 409	501 774	32% 89%
VIS/NIR FPA	Silicon PIN Diodes	M3	0.488	0.742 x 0.259	1.60 x 1.58	Ocean Color Aerosols	Low High	32 123	416 414	573 747	38% 80%
VIS/NIR FPA	Silicon PIN Diodes	M4	0.555	0.742 x 0.259	1.60 x 1.58	Ocean Color Aerosols	Low High	21 90	362 315	482 586	33% 86%
VIS/NIR FPA	Silicon PIN Diodes	I1	0.640	0.371 x 0.387	0.80 x 0.789	Imagery	Single	22	119	135	13%
VIS/NIR FPA	Silicon PIN Diodes	M5	0.672	0.742 x 0.259	1.60 x 1.58	Ocean Color Aerosols	Low High	10 68	242 360	306 450	26% 25%
VIS/NIR FPA	Silicon PIN Diodes	M6	0.746	0.742 x 0.776	1.60 x 1.58	Atmospheric Corr'n	Single	9.6	199	279	40%
VIS/NIR FPA	Silicon PIN Diodes	I2	0.865	0.371 x 0.387	0.80 x 0.789	NDVI	Single	25	150	212	41%
VIS/NIR FPA	Silicon PIN Diodes	M7	0.865	0.742 x 0.259	1.60 x 1.58	Ocean Color Aerosols	Low High	6.4 33.4	215 340	467 467	117% 37%
CCD		DNB	0.7	0.742 x 0.742	0.742 x 0.742	Imagery	Var.	6.70E-05	6	6.2	3%
S/MWIR	PV HgCdTe (HCT)	M8	1.24	0.742 x 0.776	1.60 x 1.58	Cloud Particle Size	Single	5.4	74	109	47%
S/MWIR	PV HgCdTe (HCT)	M9	1.378	0.742 x 0.776	1.60 x 1.58	Cirrus/Cloud Cover	Single	6	83	156	88%
S/MWIR	PV HgCdTe (HCT)	I3	1.61	0.371 x 0.387	0.80 x 0.789	Binary Snow Map	Single	7.3	6.0	71	1084%
S/MWIR	PV HgCdTe (HCT)	M10	1.61	0.742 x 0.776	1.60 x 1.58	Snow Fraction	Single	7.3	342	461	35%
S/MWIR	PV HgCdTe (HCT)	M11	2.25	0.742 x 0.776	1.60 x 1.58	Clouds	Single	0.12	10	14	44%
S/MWIR	PV HgCdTe (HCT)	I4	3.74	0.371 x 0.387	0.80 x 0.789	Imagery Clouds	Single	270 K	2.500	0.236	68%
S/MWIR	PV HgCdTe (HCT)	M12	3.70	0.742 x 0.776	1.60 x 1.58	SST	Single	270 K	0.396	1.039	141%
S/MWIR	PV HgCdTe (HCT)	M13	4.05	0.742 x 0.259	1.60 x 1.58	SST Fires	Low High	300 K 380 K	0.107 0.423	0.051 0.353	111% 20%
LWIR	PV HCT	M14	8.55	0.742 x 0.776	1.60 x 1.58	Cloud Top Properties	Single	270 K	0.091	0.057	60%
LWIR	PV HCT	M15	10.763	0.742 x 0.776	1.60 x 1.58	SST	Single	300 K	0.070	0.034	105%
LWIR	PV HCT	I5	11.450	0.371 x 0.387	0.80 x 0.789	Cloud Imagery	Single	210 K	1.500	1.004	49%
LWIR	PV HCT	M16	12.013	0.742 x 0.776	1.60 x 1.58	SST	Single	300 K	0.072	0.059	23%

Total of 22 spectral bands:

resolution

- **I** bands – 375 m (5)
- **M** bands – 750 m (16)
- DNB band – 750 m (1)

Day/Night Band (DNB)

Detailed information about the VIIRS Day-Night Band (DNB) and its nightglow observations:

Miller, Steven D., Cynthia L. Combs, Stanley Q. Kidder, Thomas F. Lee, 2012: Assessing Moonlight Availability for Nighttime Environmental Applications by Low-Light Visible Polar-Orbiting Satellite Sensors. *J. Atmos. Oceanic Technol.*, **29**, 538–557. doi: http://dx.doi.org/10.1175/JTECH-D-11-00192.1

Miller, S.D., Mills, S.P., Elvidge, C.D., Lindsey, D.T., Lee, T.F., Hawkins, J.D., 2012: Suomi satellite brings to light a unique frontier of nighttime environmental sensing capabilities. PNAS, vol. 109 no. 39, 15706–15711. doi: 10.1073/pnas.1207034109 (see also the supporting information of this paper)

Miller, S.D., Straka, W., III, Mills, S.P., Elvidge, C.D., Lee, T.F., Solbrig, J., Walther, A., Heidinger, A.K., Weiss, S.C., 2013: Illuminating the Capabilities of the Suomi National Polar-Orbiting Partnership (NPP) Visible Infrared Imaging Radiometer Suite (VIIRS) Day/Night Band. *Remote Sens.* 2013, *5*, 6717-6766. doi: 10.3390/rs5126717

Miller, S.D., Straka W.III., Yue J., Smith, S.M., Alexander, J., Hoffmann, L., Setvák, M., and Partain, P.T., 2015: Upper atmospheric gravity wave details revealed in nightglow satellite imagery. *PNAS* 2015, vol.112, no.49, E6728–E6735. doi: 10.1073/pnas.1508084112

Example of concentric gravity waves in nightglow („classic" case, above convective storms in Texas, 04 April 2014, 08:15 UTC)

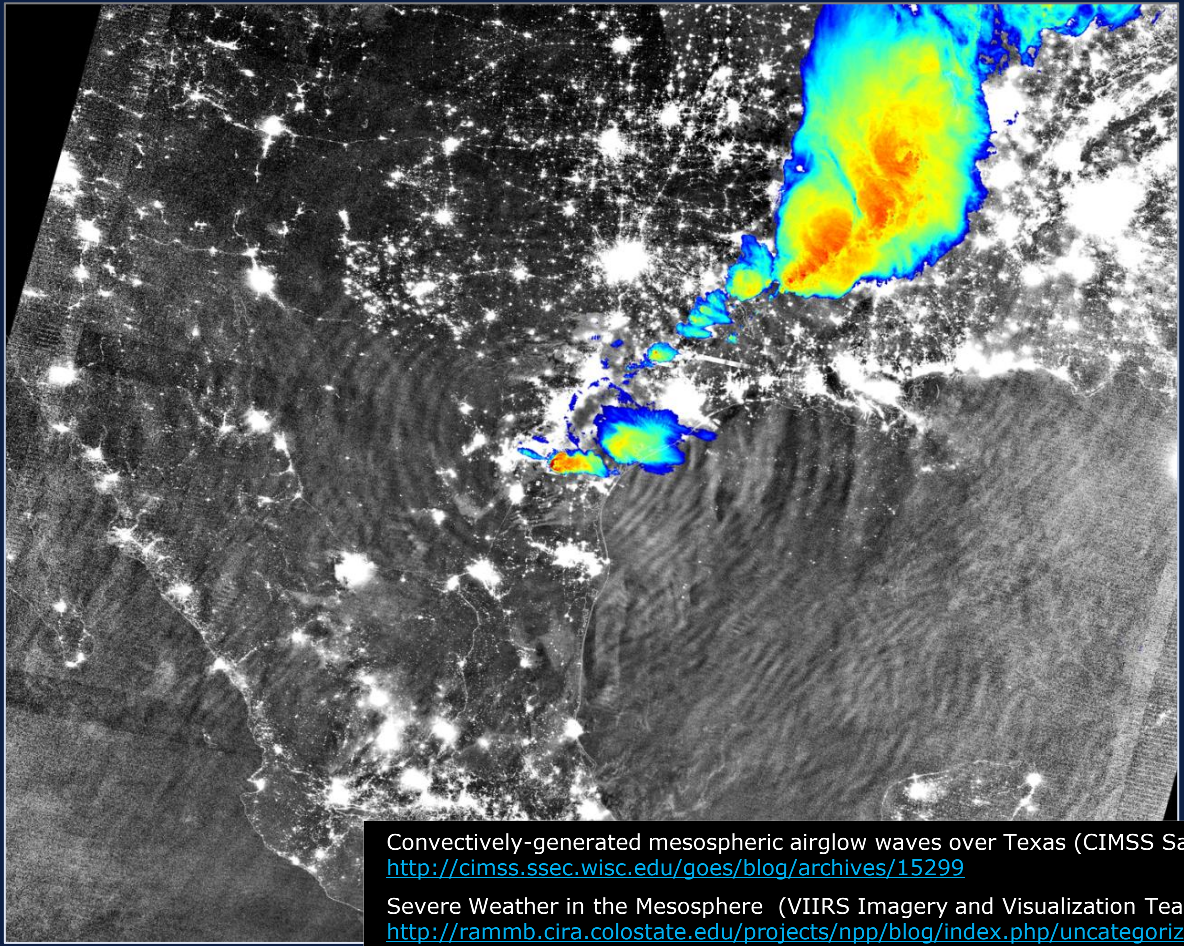

Suomi-NPP Day/Night Band and IR M15 band (190-240K)

Convectively-generated mesospheric airglow waves over Texas (CIMSS Satellite Blog)
http://cimss.ssec.wisc.edu/goes/blog/archives/15299

Severe Weather in the Mesosphere (VIIRS Imagery and Visualization Team Blog)
http://rammb.cira.colostate.edu/projects/npp/blog/index.php/uncategorized/severe-weather-in-the-mesosphere/

Concentric gravity waves (CGW) generated by convective storms in nightglow (nocturnal airglow)

The concentric gravity waves (CGW) in nightglow are in most cases evoked by vertically propagating gravity waves generated by (stronger) convective storms, their updrafts / overshooting tops.

First unambiguously documented in

Taylor, M. J., and M. A. Hapgood, 1988: Identification of a thunderstorm as a source of short period gravity waves in the upper atmospheric nightglow emissions, Planet. Space Sci., 36, s.975. DOI:10.1016/0032-0633(88)90035-9

Planet. Space Sci., Vol. 36, No. 10, pp. 975–985, 1988
Printed in Great Britain.
0032–0633/88 $3.00+0.00
Pergamon Press plc

IDENTIFICATION OF A THUNDERSTORM AS A SOURCE OF SHORT PERIOD GRAVITY WAVES IN THE UPPER ATMOSPHERIC NIGHTGLOW EMISSIONS

M. J. TAYLOR
Department of Physics, The University, Southampton SO9 5NH, U.K.

and

M. A. HAPGOOD
Rutherford Appleton Laboratory, Chilton, Didcot, Oxfordshire OX11 0QX, U.K.

(*Received in final form* 3 *February* 1988)

Abstract—A short period gravity wave train was detected by its effect on three upper atmospheric nightglow emissions, the OI 557.7 nm and Na 589.2 nm lines and the OH bands between 715 and 810 nm (Taylor *et al*., 1987, *Planet. Space Sci.* **35**, 413). Images of these emissions, which were recorded on the evening of 14 August 1980 from the Gornergrat Observatory, Switzerland (45.98°N, 7.78°E), contained high contrast wave-like structures coherent in all three emissions and exhibiting curvature. These properties have been used to identify a thunderstorm centred over southern France as the most likely source of the waves.

Recently, the source of these can be typically very easily traced, comparing the DNB images with IR bands or their combinations – either from the same satellite (same time and viewing geometry as the DNB image), or following the area of interest in geostationary IR image data (for information about evolution of the storms).

Concentric gravity waves in nightglow above Bangladesh, 27 April 2014

Jeff Dai, 2014-04-27 15:57 UTC, Tibet Plateau, China
https://www.flickr.com/photos/jeffdai/14845763849/

Concentric gravity waves in nightglow above Bangladesh, 27 April 2014

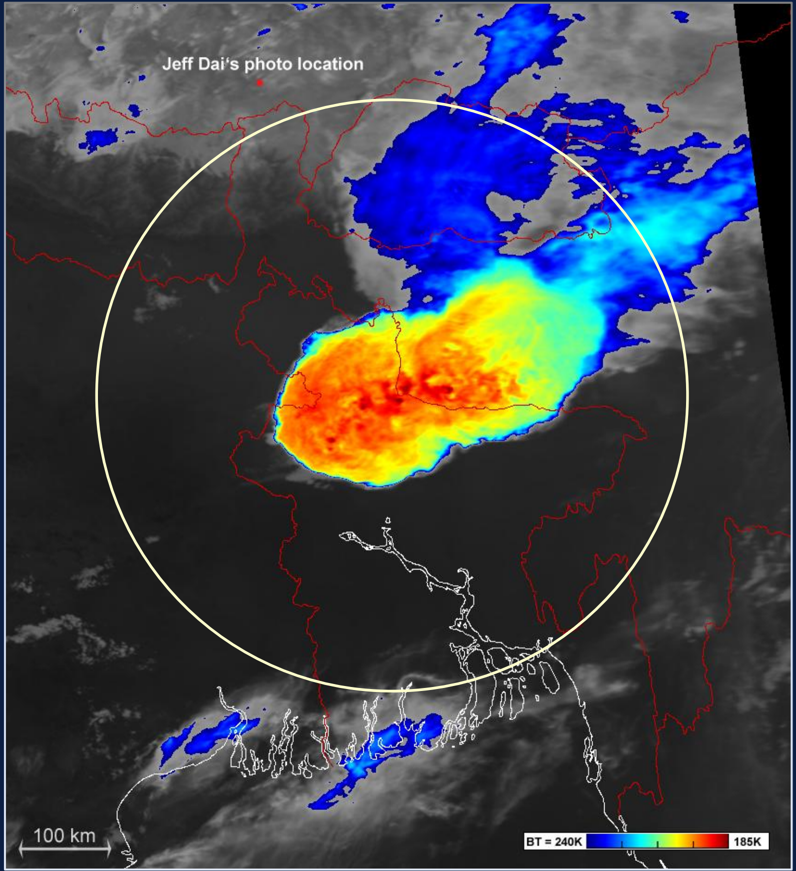

2014-04-27 15:50 UTC
Metop-2 band 4 (IR 10.5 µm)

This Metop-2 image was taken almost exactly at the same time as Jeff Dai took his famous "rippled sky" photo (previous slide) from the Tibetan Plateau in China.

This storm started to evolve about 1 hour prior to this image and Jeff Dai's observations. For evolution of these storms see the Meteosat-7 IR loop at the first of the links below.

Suomi-NPP VIIRS captured the waves in nightglow about **3.5 hours later**, when the storms were already weakening (next 3 slides).

A Kalboishakhi storm swept across northern Bangladesh on the evening of 27 April 2014 (EUMETSAT Image Library)
http://www.eumetsat.int/website/home/Images/ImageLibrary/DAT_2204046.html

Rippled airglow above Bangladesh storms (EUMETSAT Image Library)
http://www.eumetsat.int/website/home/Images/ImageLibrary/DAT_2529304.html

Concentric gravity waves in nightglow above Bangladesh, 27 April 2014

Suomi-NPP VIIRS
19:35 UTC

DNB image

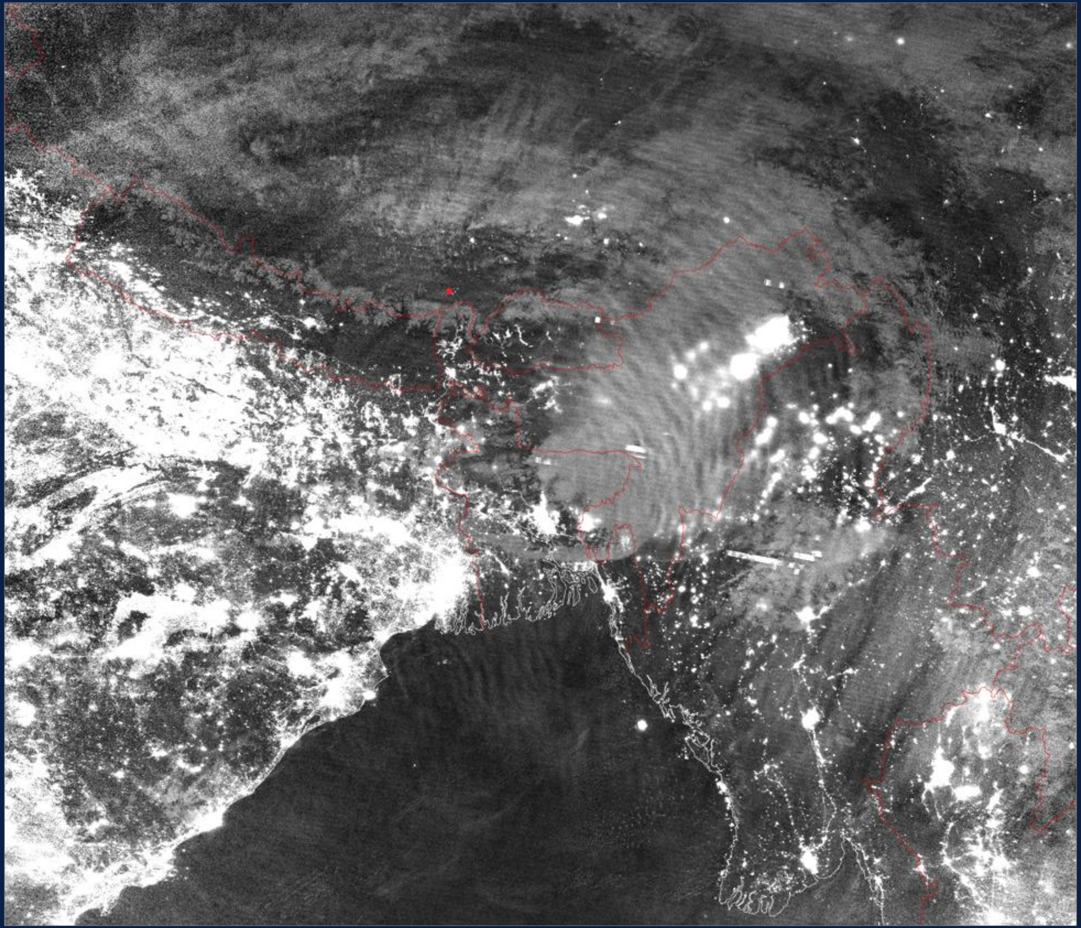

Concentric gravity waves in nightglow above Bangladesh, 27 April 2014

Suomi-NPP VIIRS
19:35 UTC

M15 (IR 10.7 μm)
BT 200 – 240 K

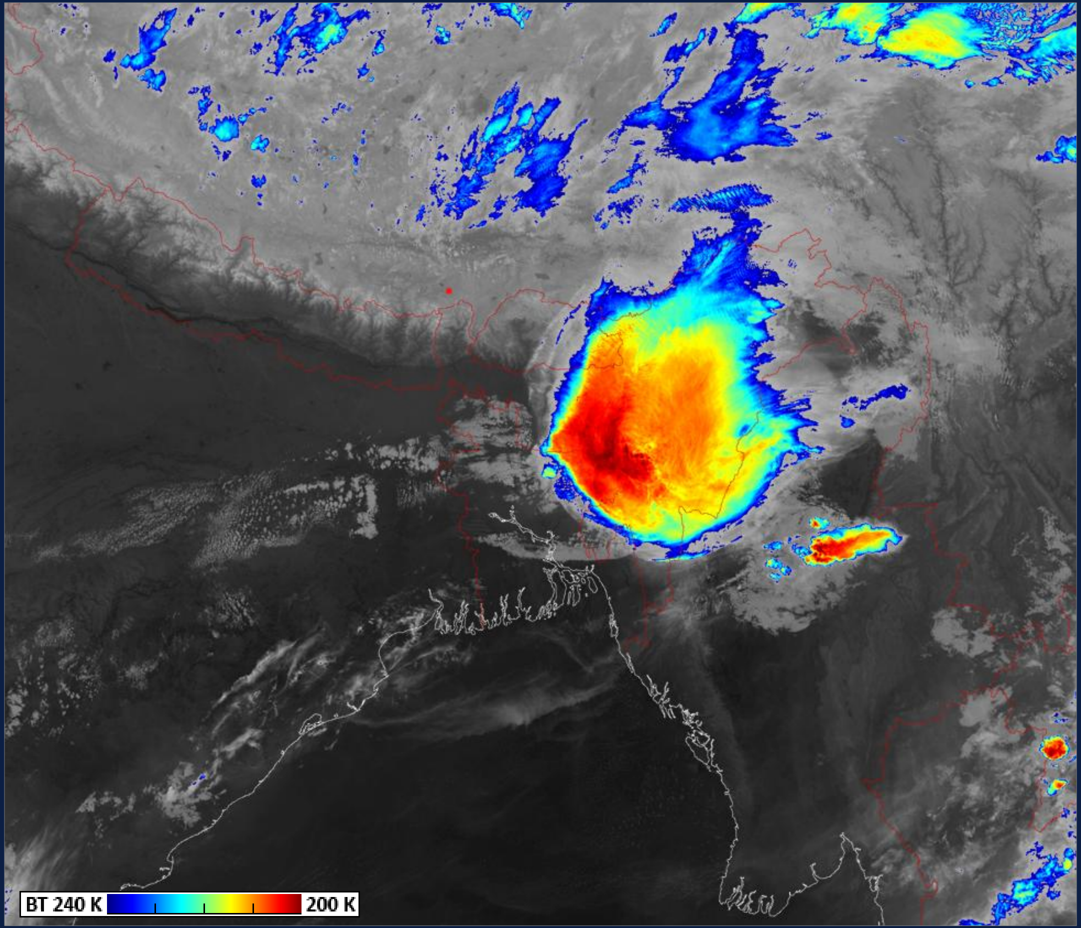

Concentric gravity waves in nightglow above Bangladesh, 27 April 2014

Suomi-NPP VIIRS
16:35 UTC

M12, M15 & M16
night microphysical
RGB product

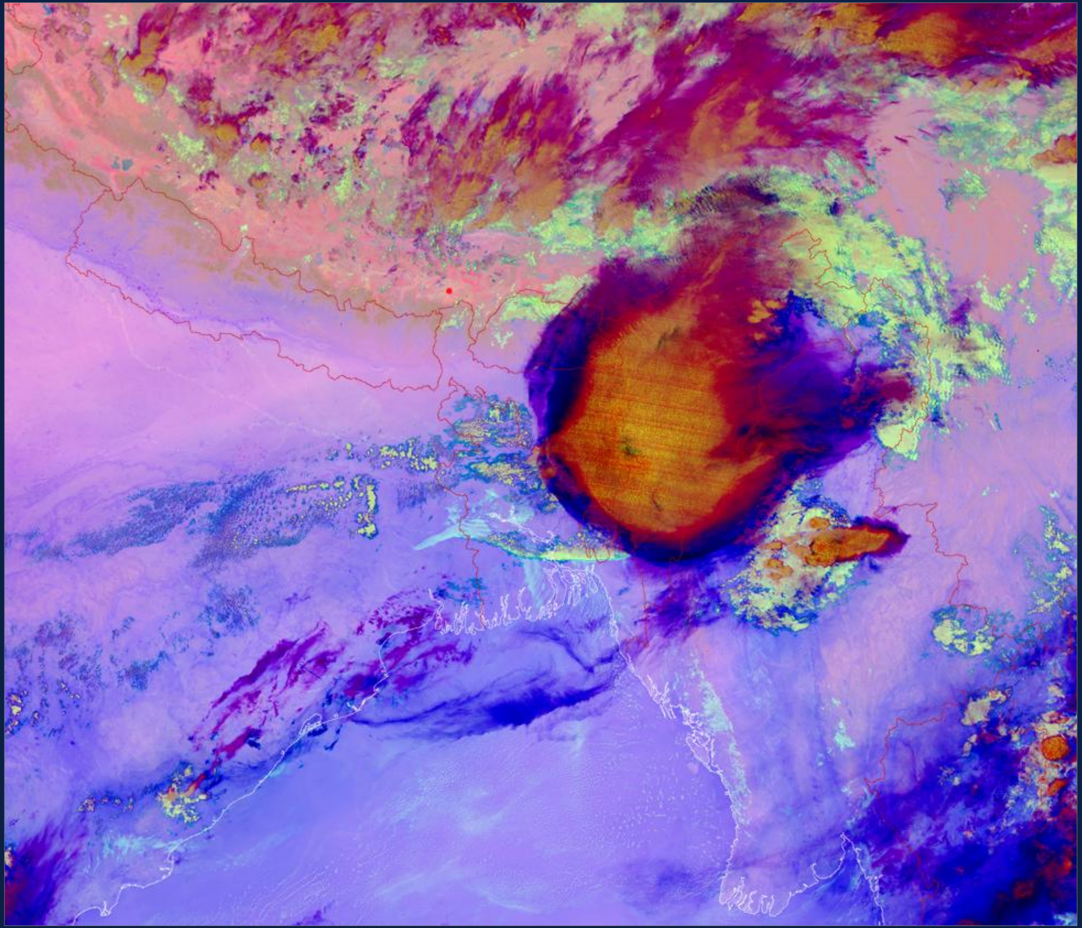

Advantage of using similar RGB products as compared to single IR band images:

- easier detection of low clouds above cold ground
- easier detection of thin transparent cirrus
- basic cloud microphysics interpretation
- detection of dust storms in deserts and other arid areas

Nighttime DNB imagery @ NASA EOSDIS Worldview – from global scale to details of various local phenomena

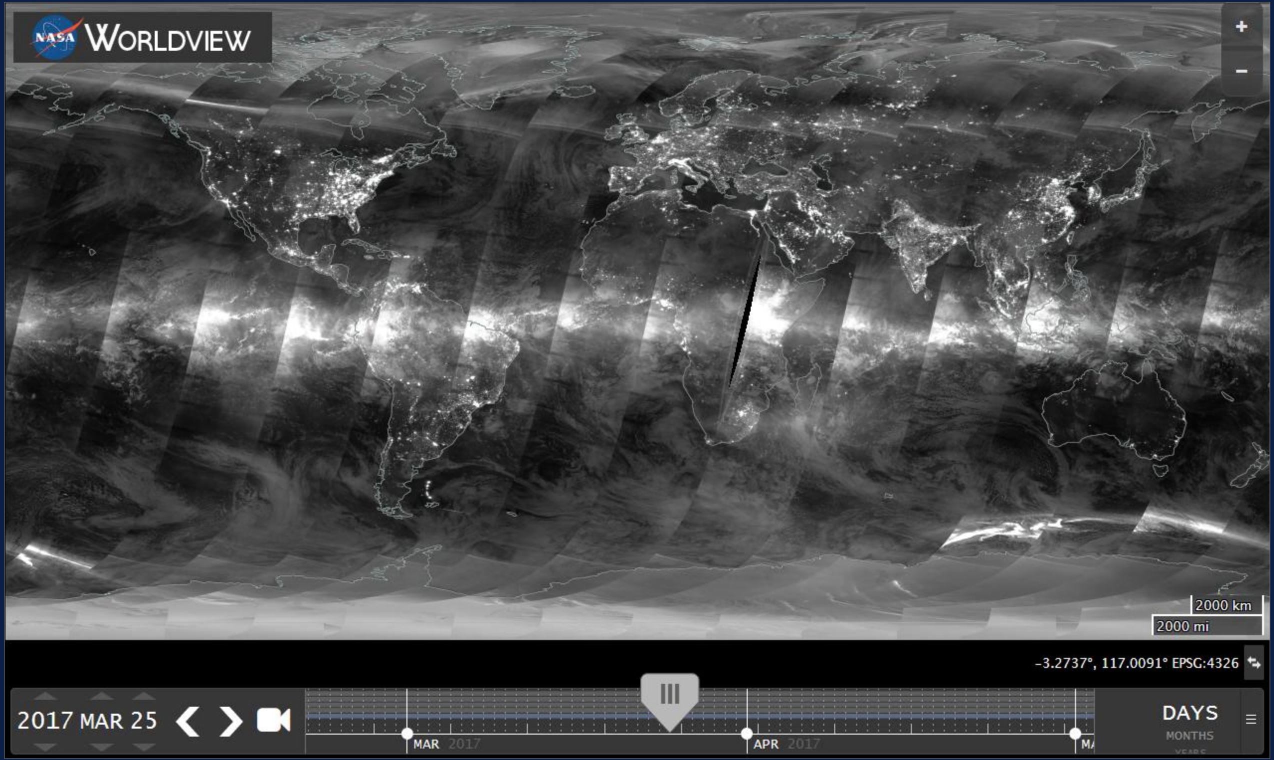

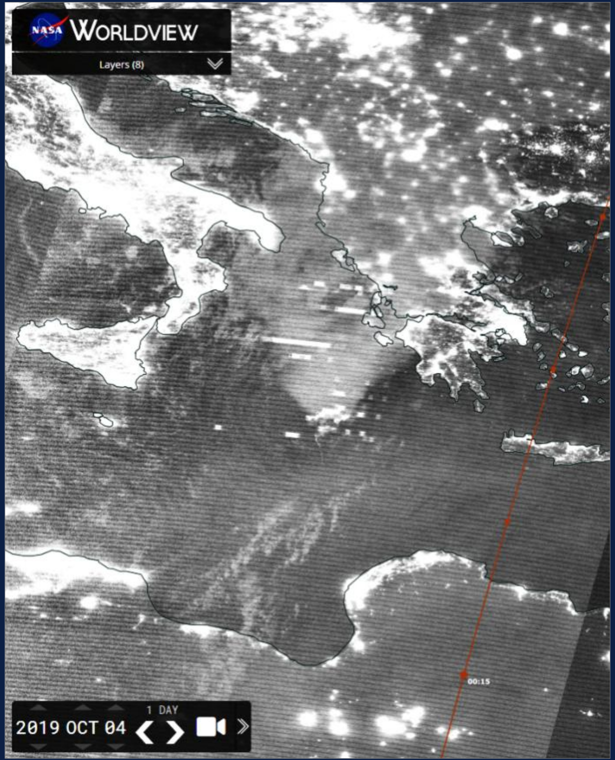

NASA Worldview: worldview.earthdata.nasa.gov/

(DNB images available here since 30 November 2016)

Appearance of concentric gravity waves in nightglow, as observed in DNB

Big diversity of concentric gravity waves observed in nightglow, generated by convective storms:

- young (fresh) CGWs … typically closed patterns (full „circle”), with well-defined individual waves, smaller horizontal extent, located above still active storm;
- mature CGW … larger horizontal extent (up to ~ 2000 – 3000 km from the „parent” storm), waves closer to their source storm still well defined, while the older (?), more distant waves are beginning to fade out, mostly lower frequency, diffuse appearance;
- old, dissipating waves – usually their parent storm already gone, without any well-defined CGW near the dissipating storm or its remains, diffuse appearance;
- open versus closed patterns: most of mature or old CGW spreading into limited sectors only, with no wave patterns at one of its sides. Typical e.g. for storms at African northern subtropics – typically missing waves at more distant southern sector of these (towards the equator).

Examples of various forms of concentric gravity waves in nightglow, as observed in DNB

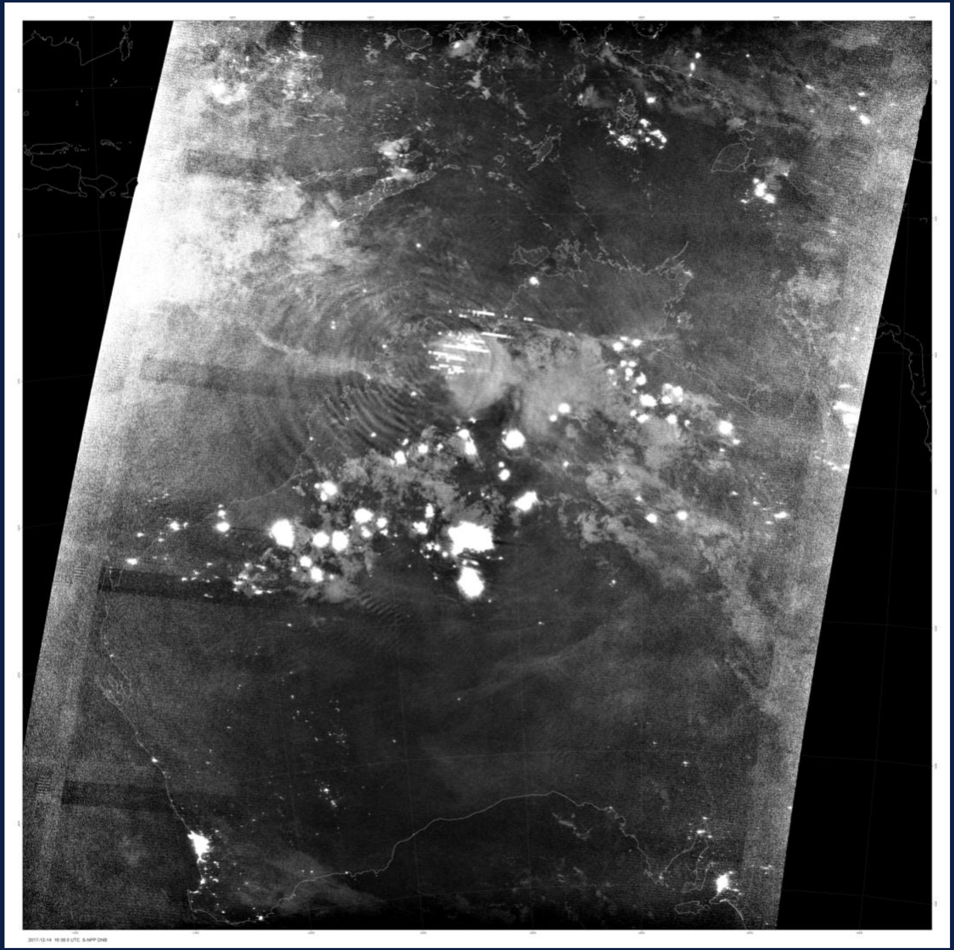

2017-12-14 16:38 UTC, Australia (S-NPP)

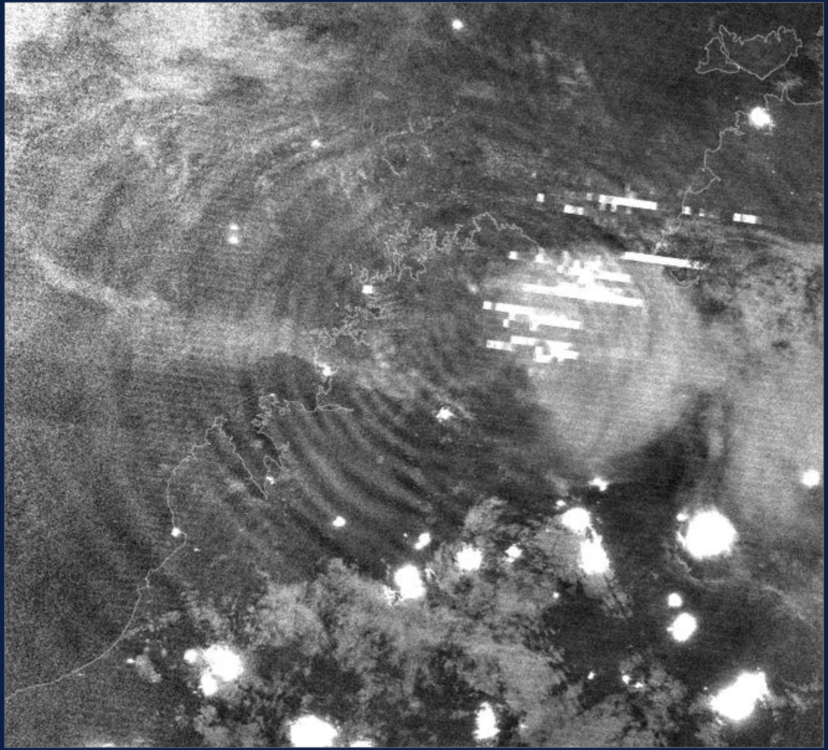

(zoom)

Examples of various forms of concentric gravity waves in nightglow, as observed in DNB

2019-10-04 01:03 UTC
Mediterranean Sea
NOAA-20

Examples of various forms of concentric gravity waves in nightglow, as observed in DNB

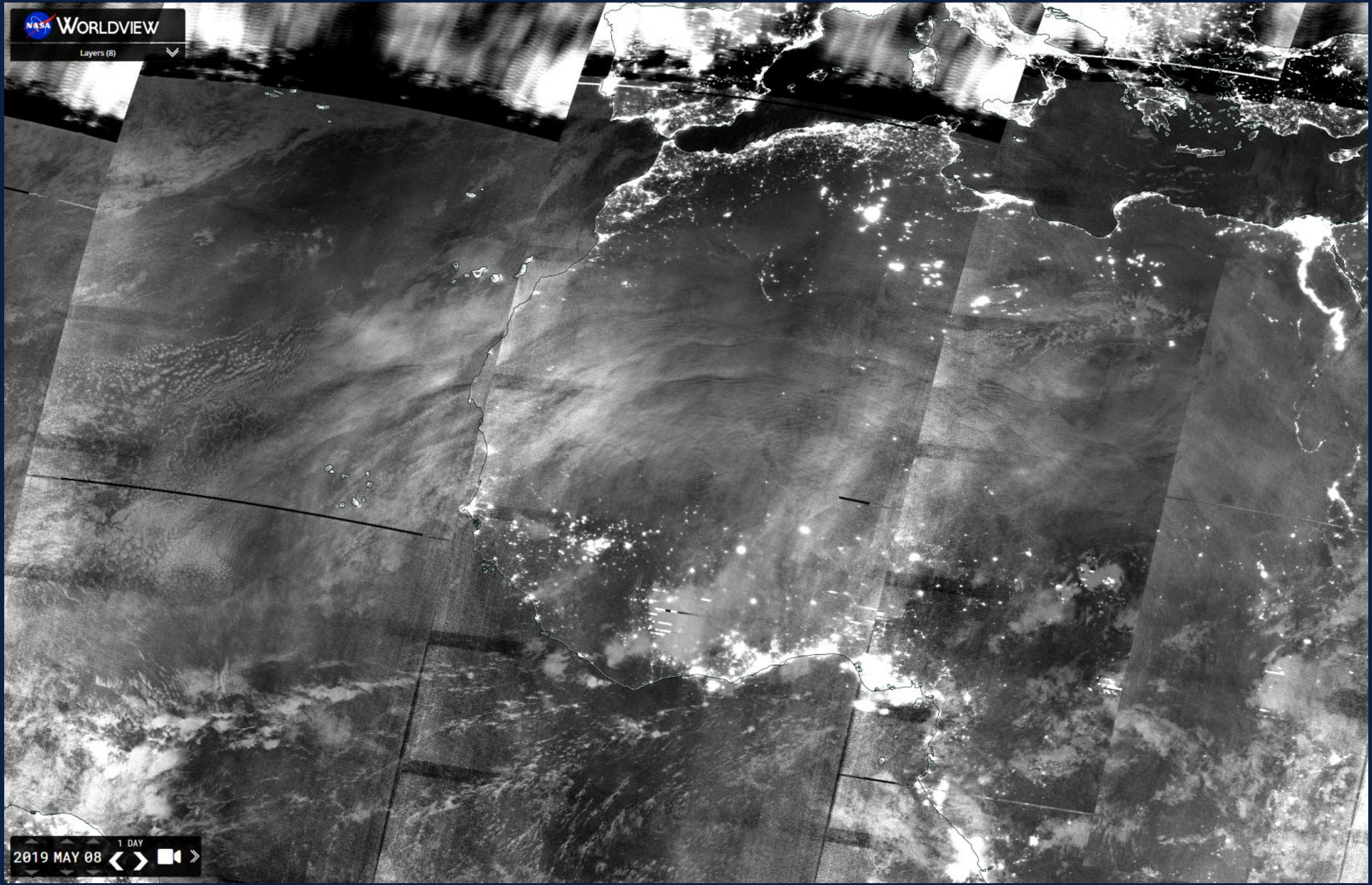

2019-05-08 00–03 UTC,
NW Africa (S-NPP)

Possible interpretation problems and ambiguities when correlating the CGWs in nightglow (in DNB) with tropospheric phenomena (in the IR bands)

- Parallax shift of the airglow features in DNB with respect to the ground or lower atmospheric layers (e.g. cloud tops of convective storms);
- duration of vertical propagation of the gravity waves from their low-level sources up to the airglow layers – the source can move, weaken or even vanish before the gravity waves reach the airglow levels and modify them;
- influence of stratosphere and mesosphere on storm-generated gravity waves during their propagation upwards – attenuation of the waves, their shift (vertical tilt), primary versus secondary GW, …
- persistence of the airglow waves after decay of their source (e.g. convective storm) which has evoked these, combined with possible advection of the airglow layers and displacement of the source itself (e.g. propagation of the storms).

- **Lack of similar instrument in the GEO orbit – no space-borne, continuous information on evolution of CGW in nightglow and their variability throughout the whole night.**

Summary of CGW cases detected in DNB (till 25 Oct 2019)

CGW (and partial CGW) detections in nightglow in **VIIRS DNB** data (Suomi-NPP and NOAA-20)					
REGION	2013-2016	2017	2018	2019	total:
Mediterranean region (including all coastal areas)	4	2	4	3	13
Africa (including east Atlantic, west Indian ocean)	24	19	14	16	73
North America and NE Pacific	1	5	0	6	12
South America and SE Pacific	0	2	3	0	5
Australia (and adjacent seas/oceans)	0	1	6	5	12
East Asia (east of India, and adjacent seas/oceans)	2	0	2	3	7
SW Asia (incl. India and Arab Peninsula, and adj. seas/ocean)	1	4	1	3	9
total:	32	33	30	36	131

Geographical distribution of DNB CWG detections: most of these from north subtropics of Africa. However, the geographical distribution of DNB detections is strongly compromised and biased by a significant non-meteorological factor: heavy light pollution in some of the otherwise storm-rich areas, such as the U.S., Europe or China, where the bright background adversely impacts DNB-based CWG detection.

While the cases during 2013 – 2016 were gathered unmethodically (based on scrutiny of DNB imagery in correlation with deep convection as identified in the VIIRS and Meteosat Second Generation (MSG) infrared band imagery), the cases from 2017 – 2019 result from a global systematic survey of NPP DNB imagery, available through NASA's EOSDIS Worldview service since 30 November 2016.

Gravity waves in AIRS data (Atmospheric Infrared Sounder, Aqua satellite)

Simultaneous observations of CGW observed in DNB (85–100 km) and AIRS 4.3 μm radiance (30-40 km) bands - namely above tropical cyclones, e.g.:

- Jia Yue, Steven D.Miller, Lars Hoffmann, William C. StrakaIII, 2014: Stratospheric and mesospheric concentric gravity waves over tropical cyclone Mahasen: Joint AIRS and VIIRS satellite observations. http://dx.doi.org/10.1016/j.jastp.2014.07.003
- Gong, Jie; Yue, Jia; and Wu, Dong L., 2015: Global survey of concentric gravity waves in AIRS images and ECMWF analysis. *NASA Publications. Paper 157.* http://digitalcommons.unl.edu/nasapub/157
- L.Hoffmann, M.J.Alexander, C.Clerbaux, A.W.Grimsdell, C.I.Meyer, T.Rößler, and B.Tournier, 2014: Intercomparison of stratospheric gravity wave observations with AIRS and IASI. Atmos. Meas. Tech., 7, 4517–4537, 2014. doi:10.5194/amt-7-4517-2014

Our study: survey of all collected DNB-based CGW cases in nightglow for presence of corresponding (concentric) gravity waves in the AIRS data.

Simple approach – use of the original radiances only. Probably not as efficient as other, more advanced methods described in the studies above, but easy and fast.

Example of concentric gravity waves in nightglow (left, ground-based photo), and in the upper stratosphere, in AIRS data (right)

Bangladesh, 27 April 2014

Jeff Dai, 2014-04-27 15:57 UTC, Tibet Plateau, China
https://www.flickr.com/photos/jeffdai/14845763849/

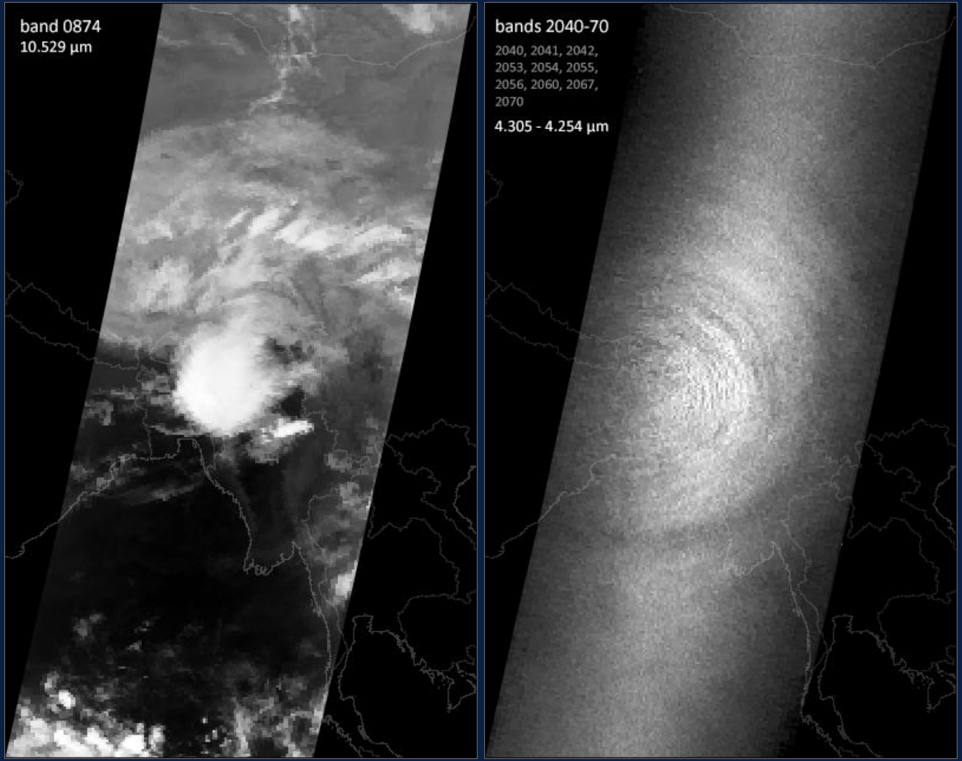

AIRS (Aqua) 19:29 – 19:41 UTC

AIRS instrument (Atmospheric Infrared Sounder, Aqua satellite)

Example of AIRS daily L1B IR global coverage (descending passes)

AIRS sounder:

2378 individual bands

3.74 – 4.61 μm
6.20 – 8.22 μm
8.80 – 15.4 μm

swath width: 1650 km

IFOV 1.1° ~ 13.5 km footprint at nadir

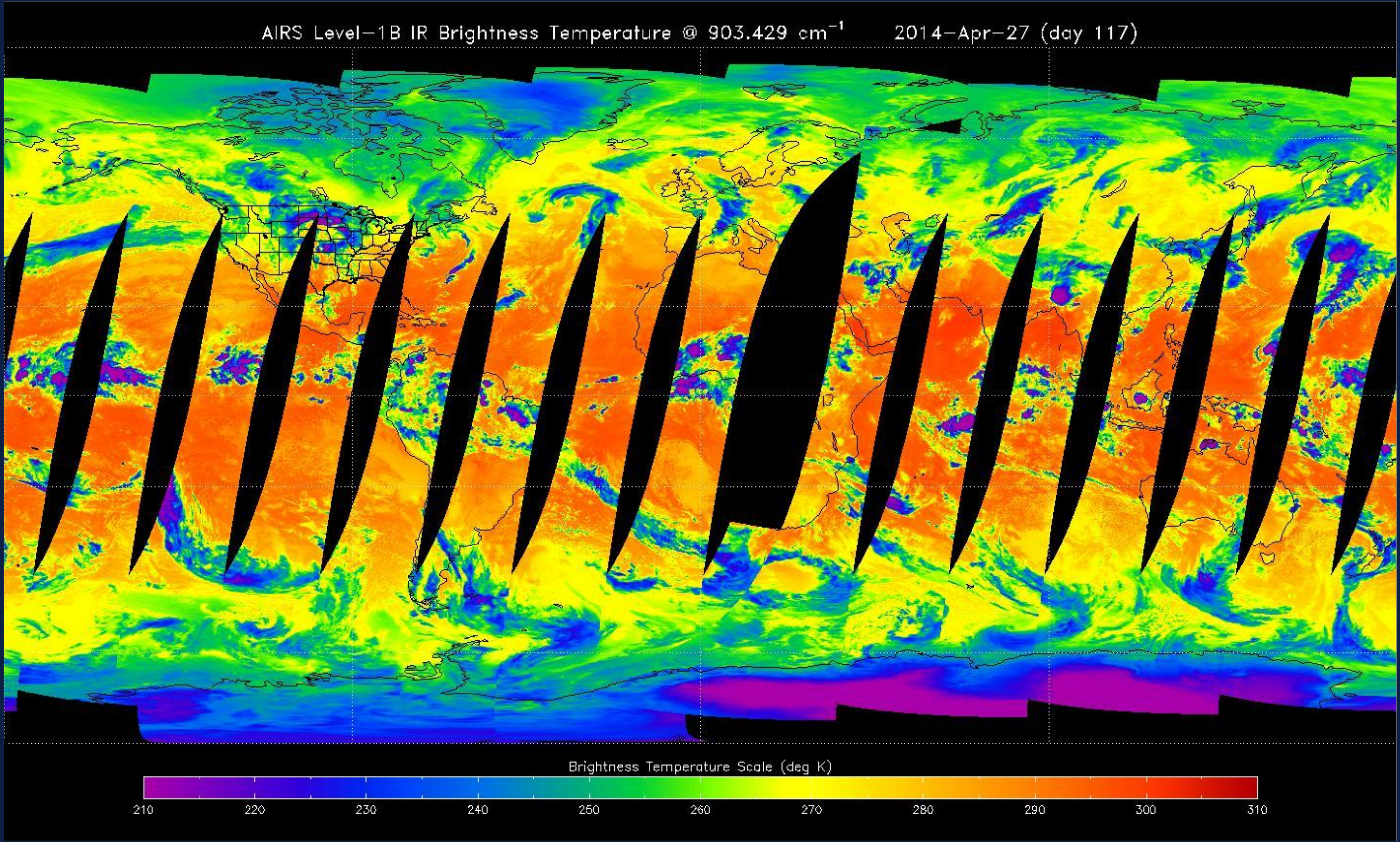

Limited geographical coverage by AIRS data at lower latitudes – many of the DNB concentric GW cases either in the gaps between individual AIRS overpasses, or at their edge.

AIRS instrument (Atmospheric Infrared Sounder, Aqua satellite)

Bangladesh, 27 April 2014

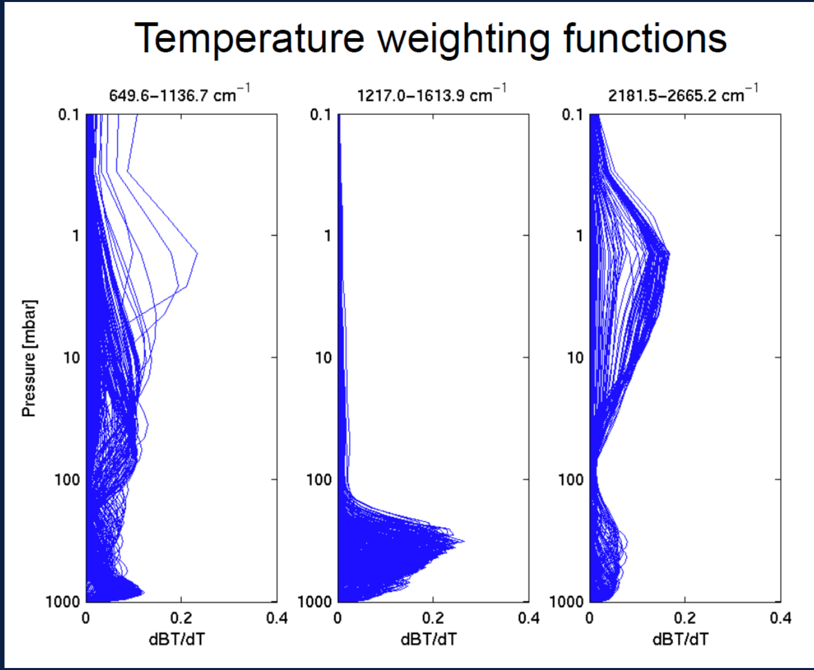

General example of AIRS weighting functions (Jacobians)
source: AIRS Instrument Characteristics (available here)

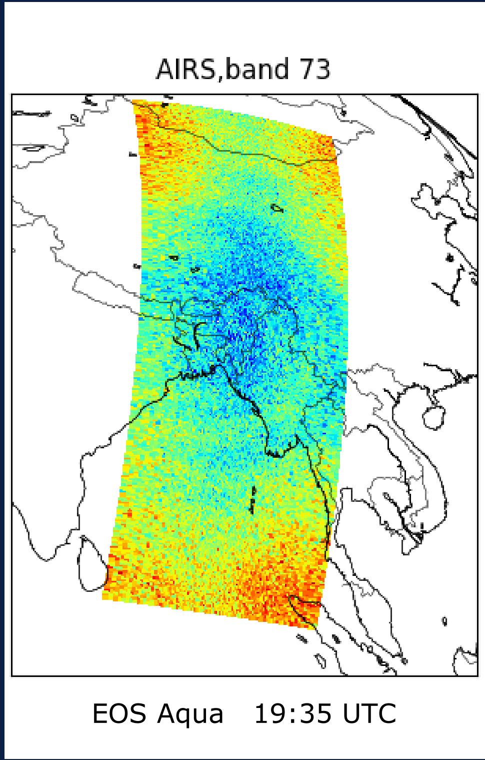

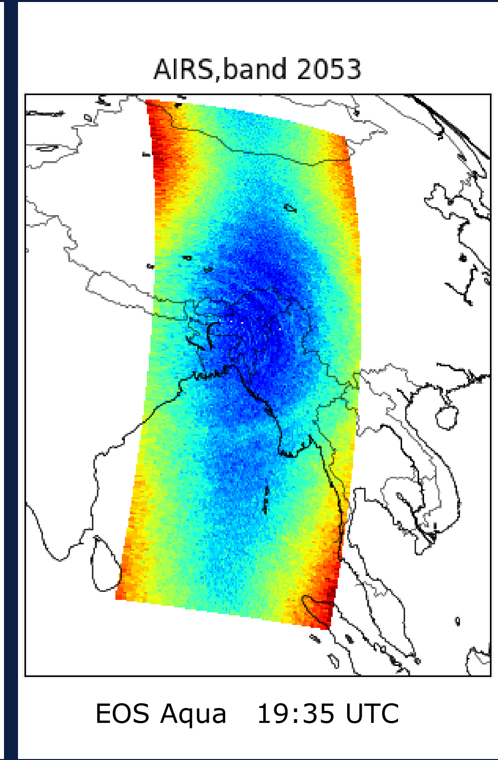

27 April 2014, AIRS bands 73 and 2053.

For the 27 April 2014 case, CGW detected in bands **73 – 76** (14.986 – 14.969 µm) , and **2030 – 2060** (4.323 – 4.271 µm).

AIRS (Aqua, 19:35 UTC)

Bangladesh, 27 April 2014

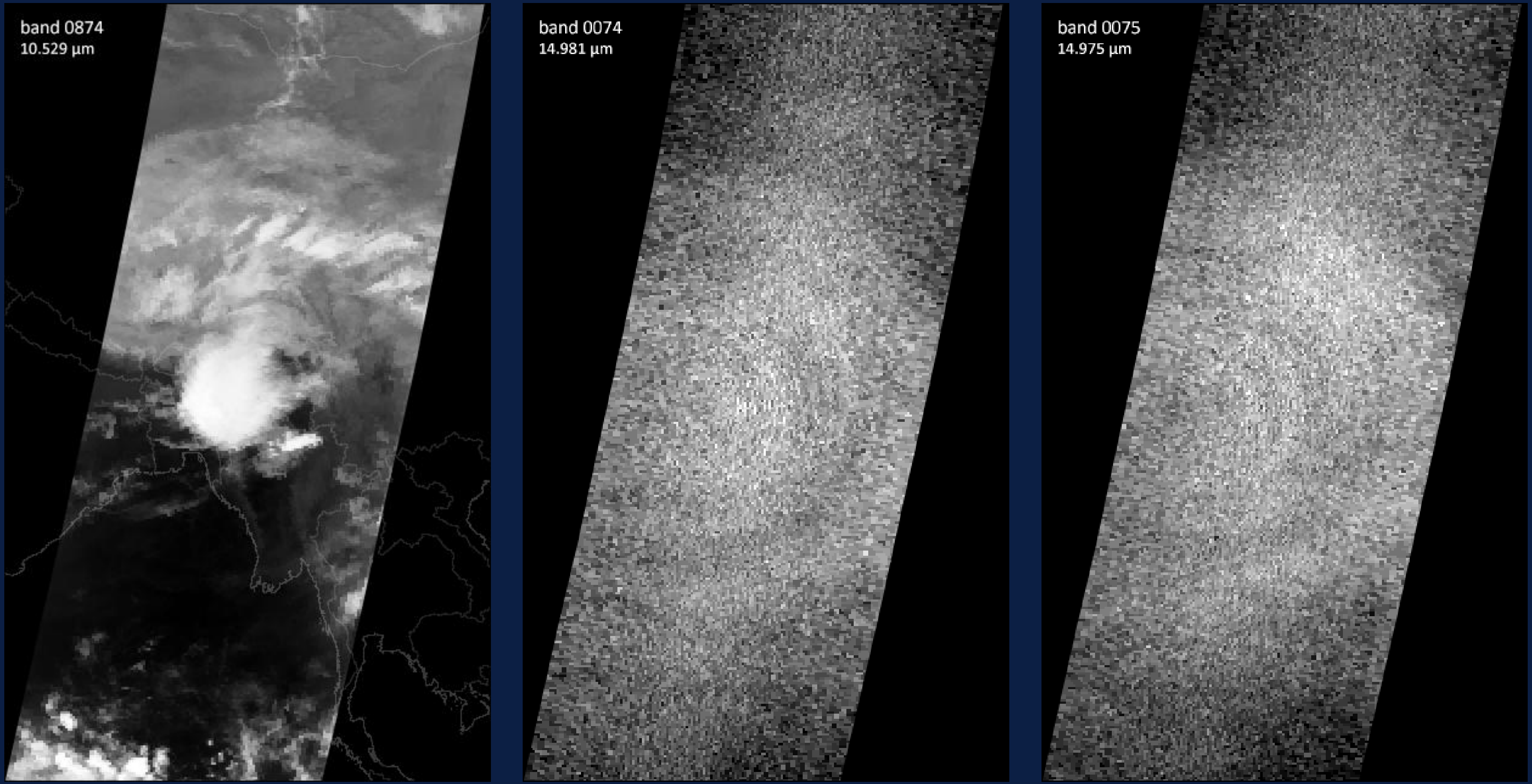

AIRS (Aqua, 19:35 UTC)

Bangladesh, 27 April 2014

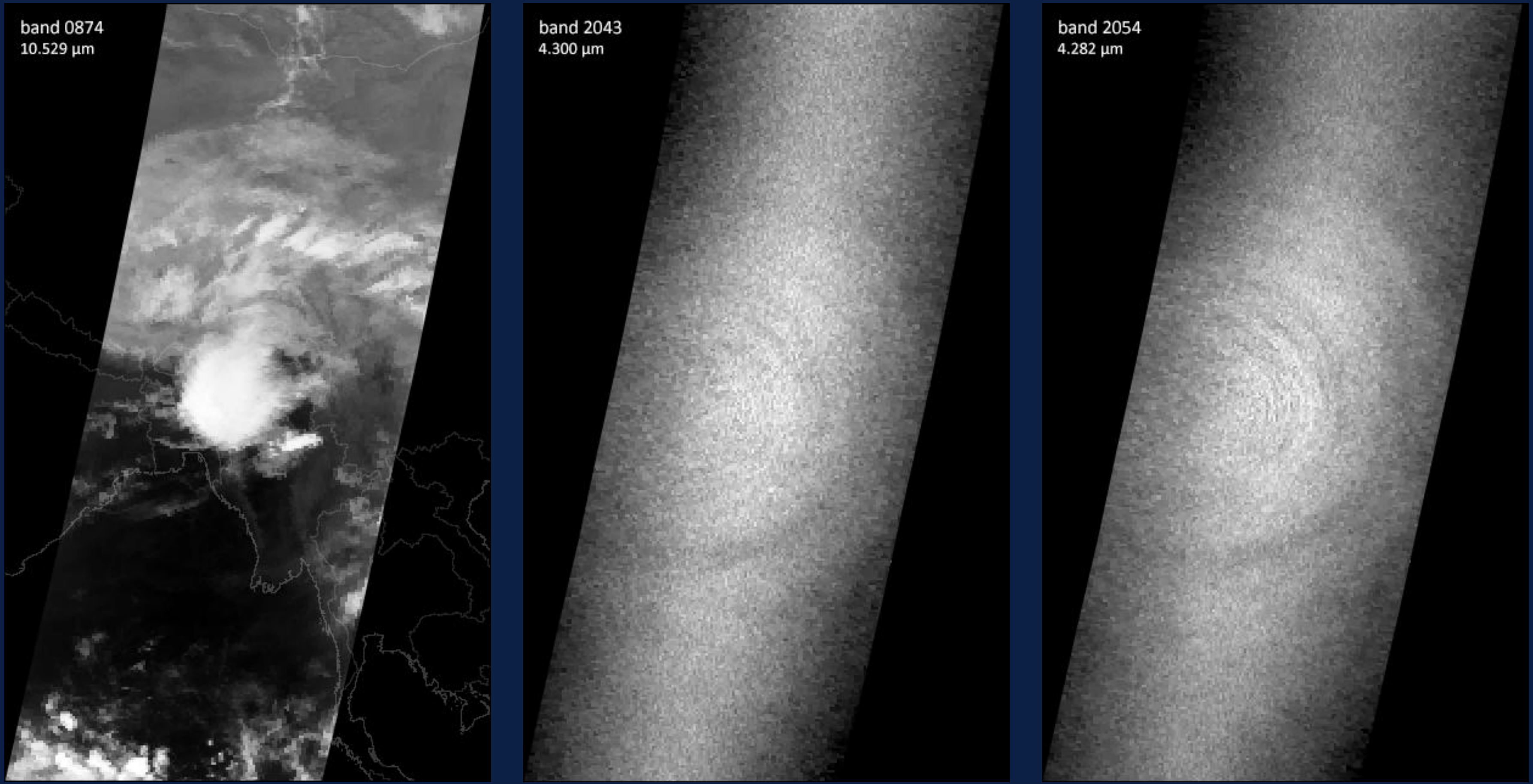

AIRS (Aqua, 19:35 UTC)

Bangladesh, 27 April 2014

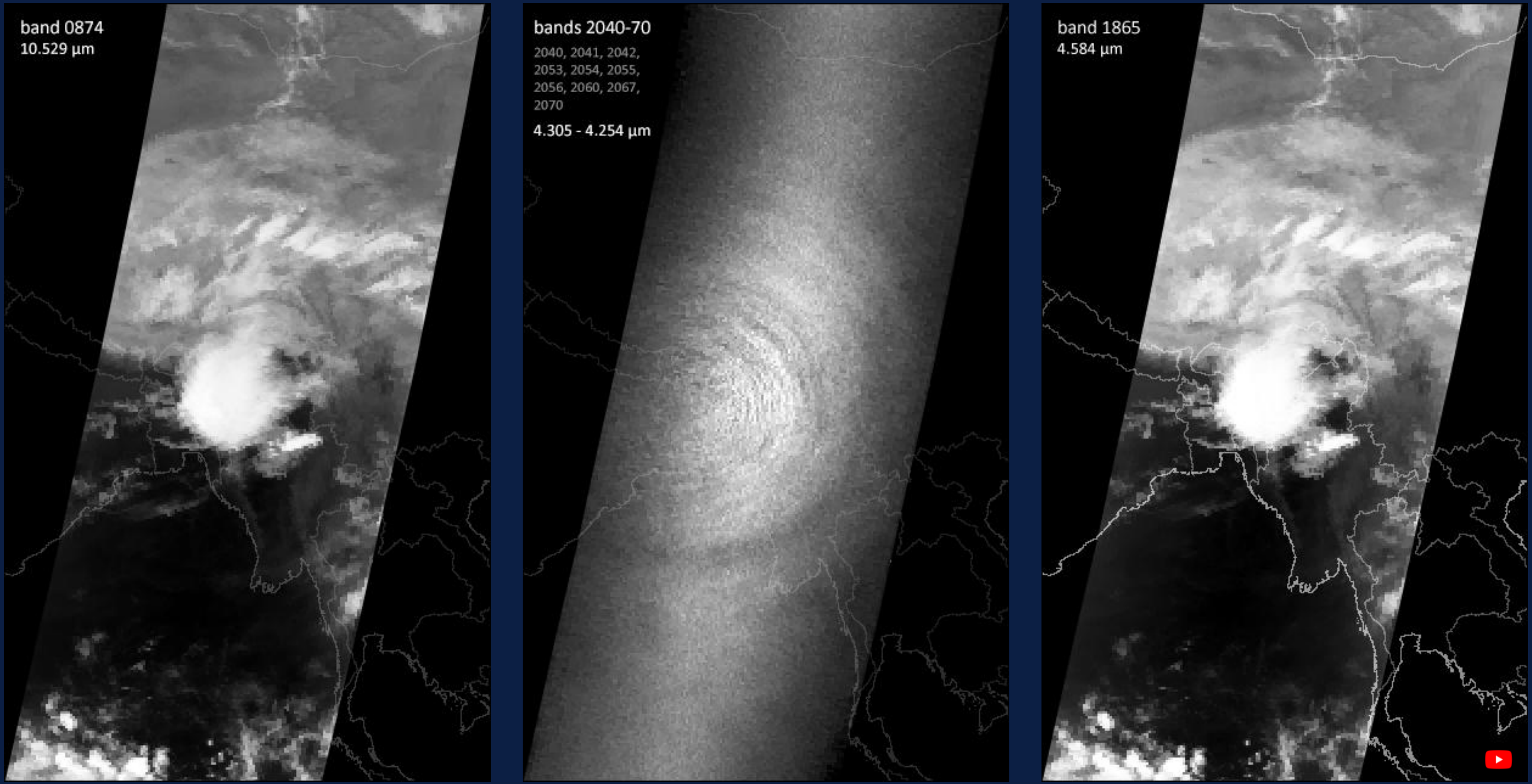

IASI – Infrared Atmospheric Sounding Interferometer, Metop 1, 2 & 3 satellites

Bangladesh, 27 April 2014

IASI swath width ~ 2200 km
horizontal resolution 12 / 25 km

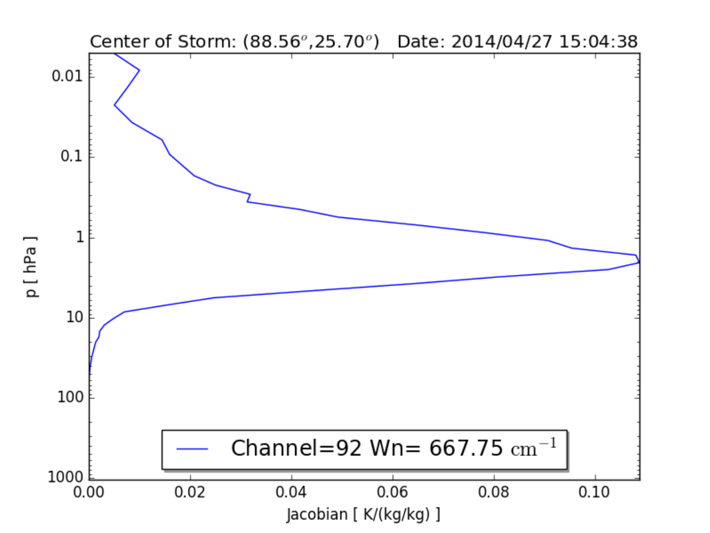

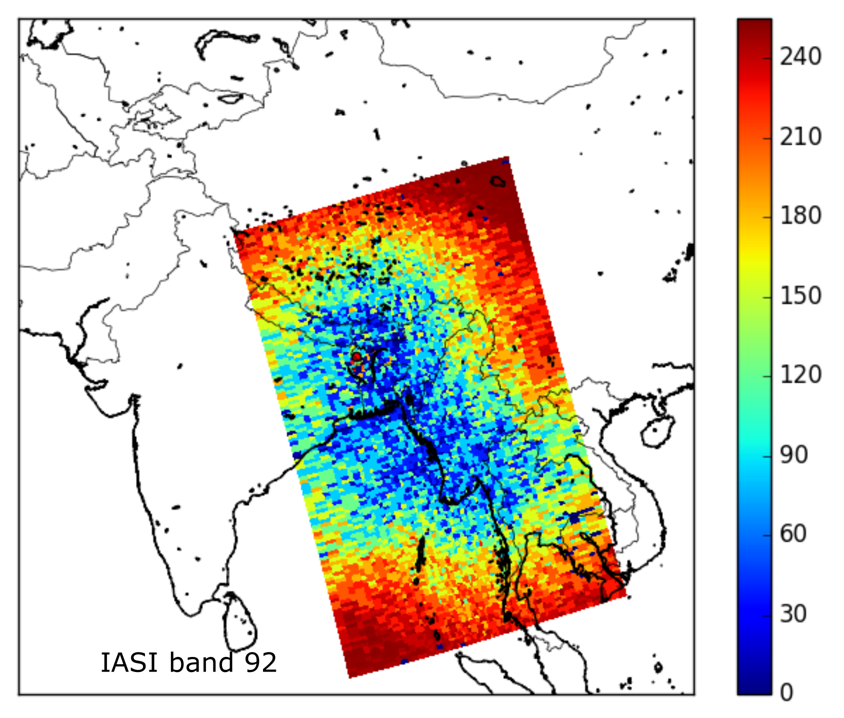

IASI Metop-1, 27 April 2014 15:05 UTC, band 92 (14.976 μm).

Example of weak concentric gravity waves in AIRS data

2018-06-16 01:36 UTC, Aqua AIRS, NW Africa

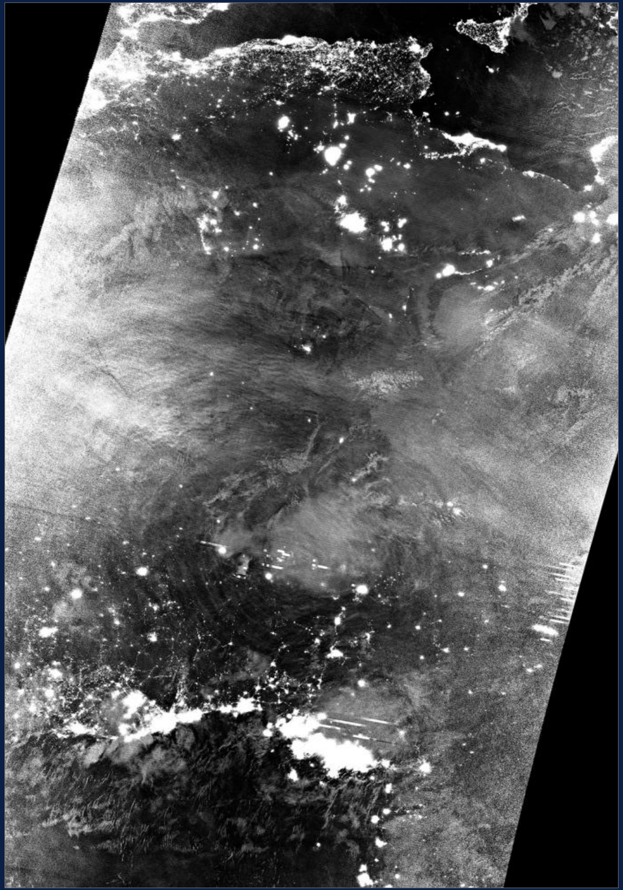

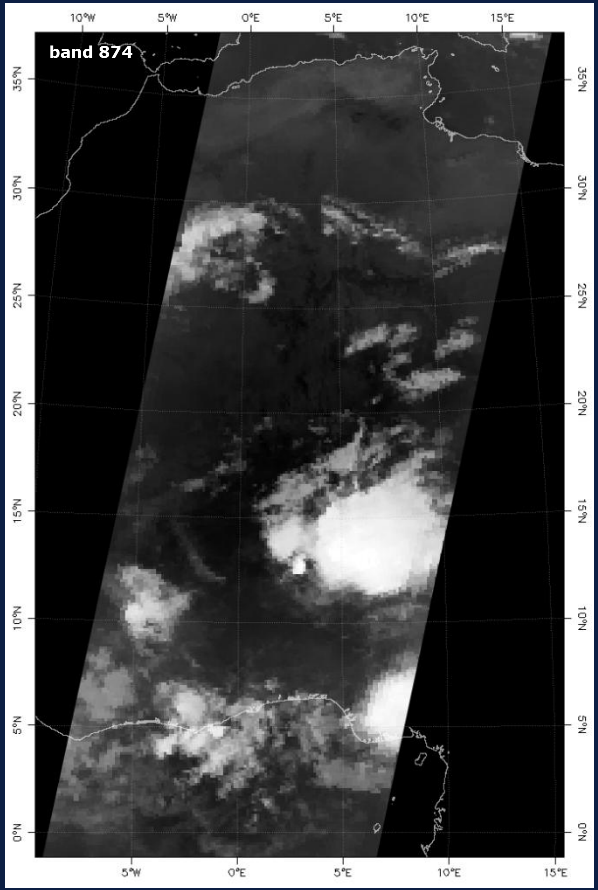

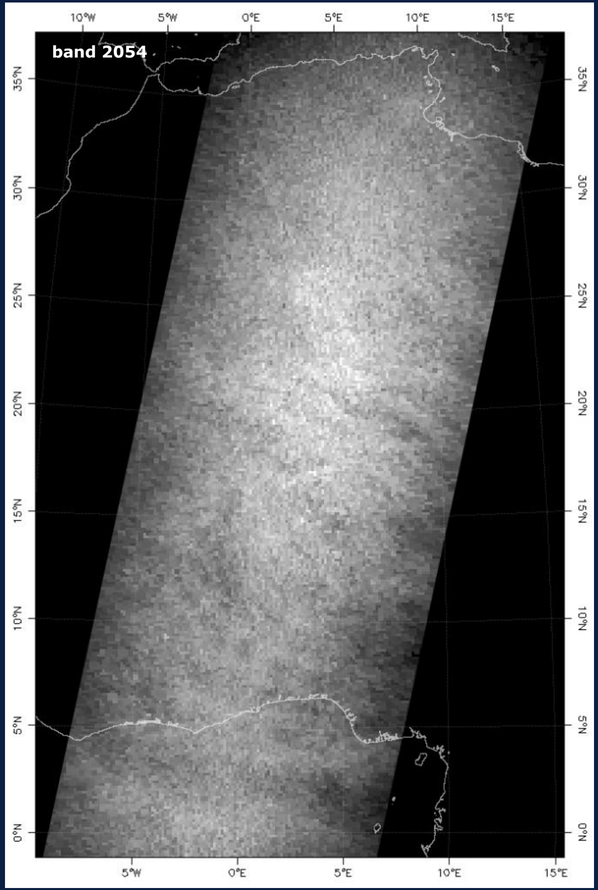

2018-06-16 01:15 UTC, NOAA-20, DNB, NW Africa

Other examples of (concentric) gravity waves in AIRS data

2017-10-19 05:05 UTC, Aqua AIRS, Argentina

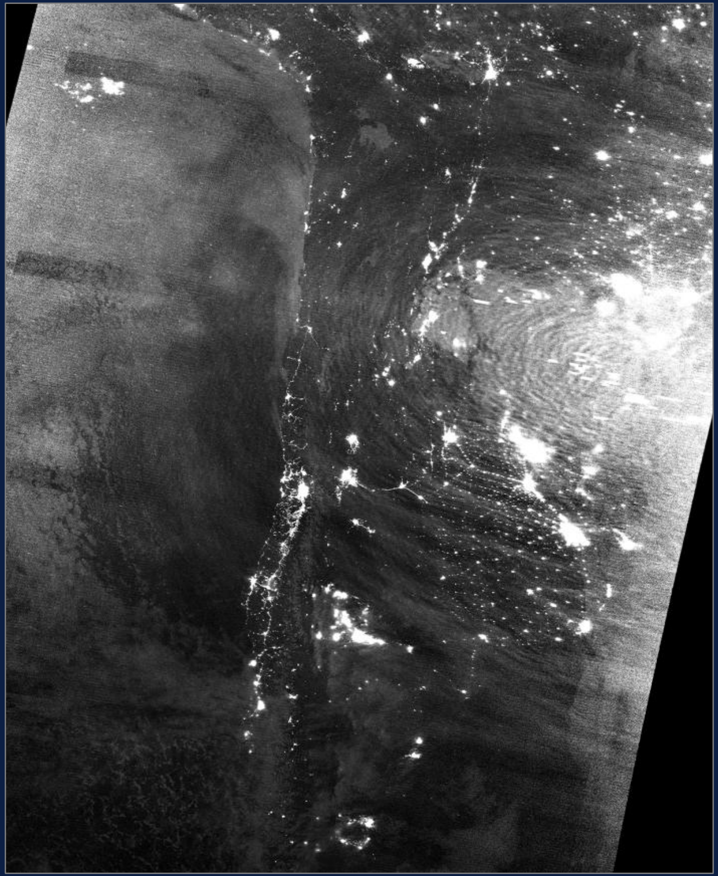

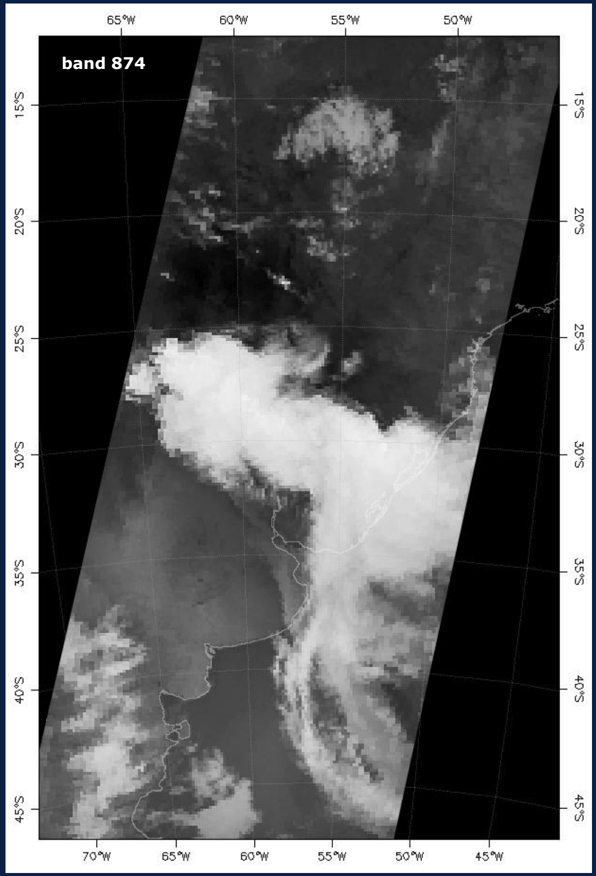

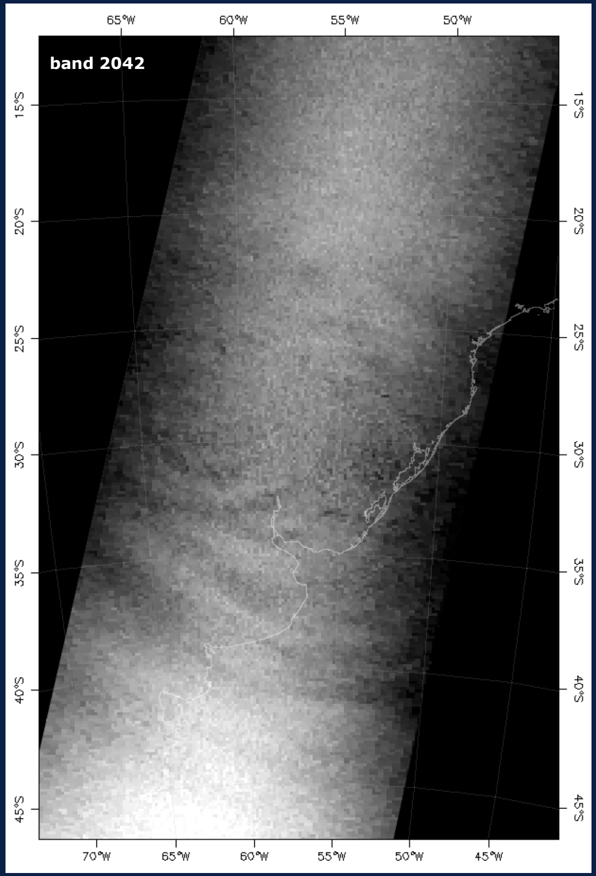

2017-10-19 05:43 UTC, S-NPP DNB, Argentina

Other examples of (concentric) gravity waves in AIRS data

2019-01-03 16:27 UTC, Aqua AIRS, Australia

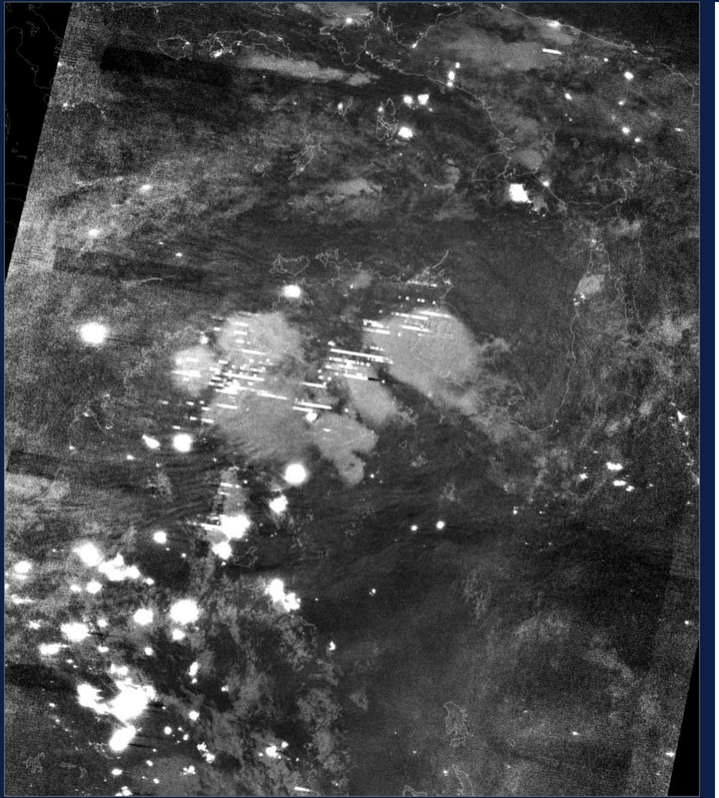

2019-01-03 16:20 UTC, S-NPP DNB, Australia

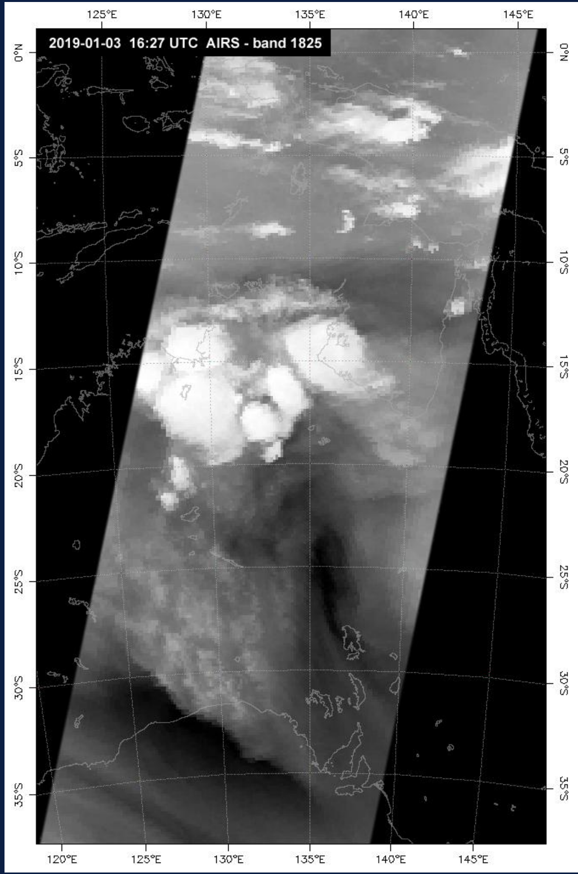

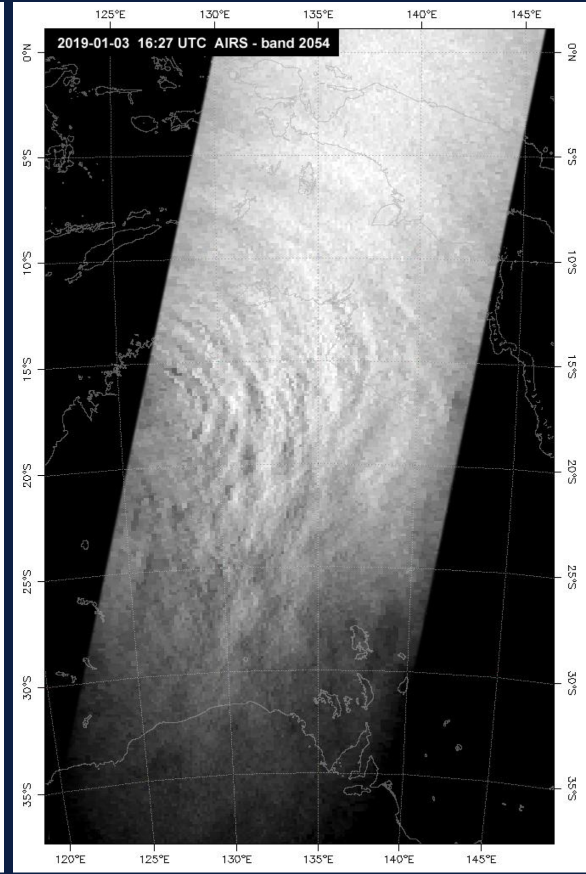

Other examples of (concentric) gravity waves in AIRS data

2019-01-12 16:22 UTC, Aqua AIRS, Australia

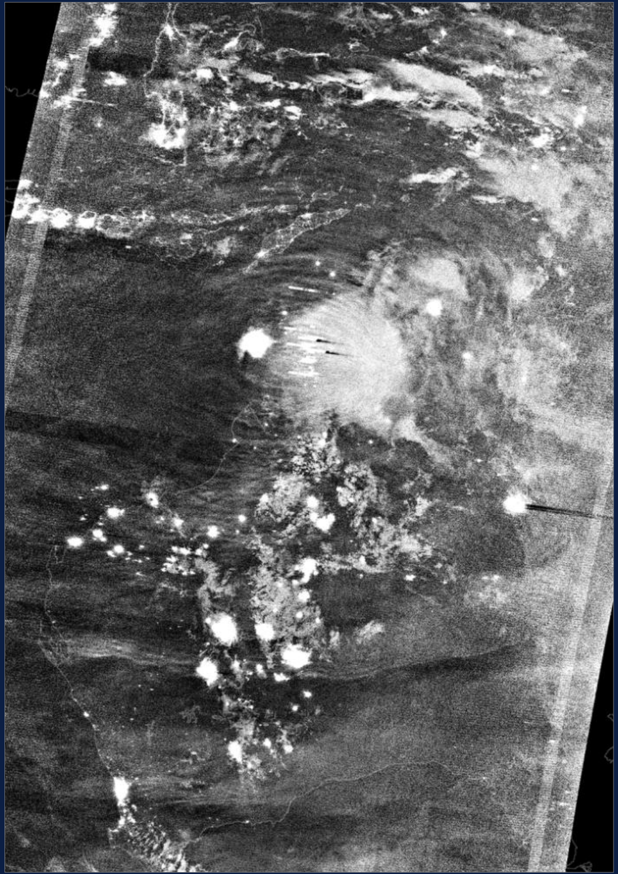

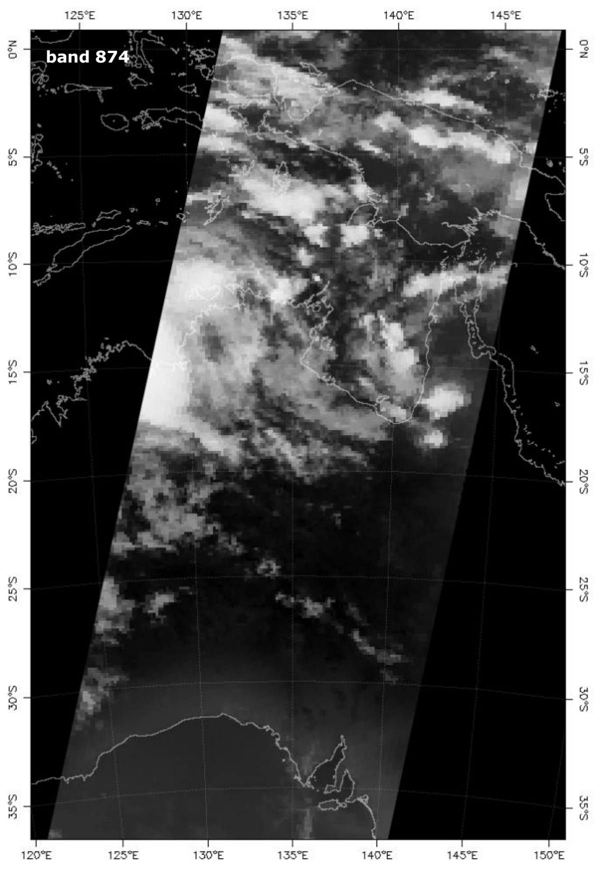

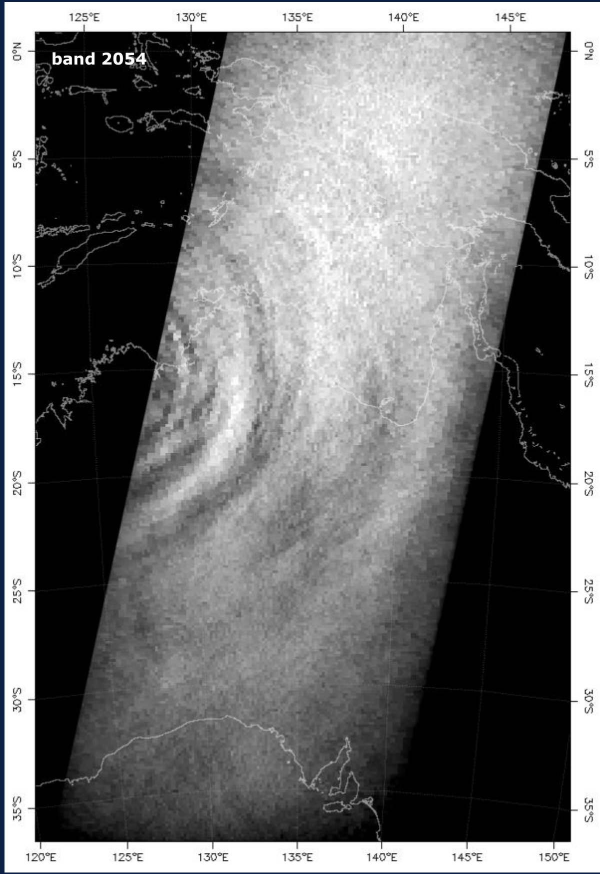

2019-01-12 16:51 UTC, S-NPP DNB, Australia

CGW (and partial CGW) detections in nightglow in **VIIRS DNB** data (Suomi-NPP and NOAA-20)					
REGION	2013-2016	2017	2018	2019	total:
Mediterranean region (including all coastal areas)	4	2	4	3	13
Africa (including east Atlantic, west Indian ocean)	24	19	14	16	73
North America and NE Pacific	1	5	0	6	12
South America and SE Pacific	0	2	3	0	5
Australia (and adjacent seas/oceans)	0	1	6	5	12
East Asia (east of India, and adjacent seas/oceans)	2	0	2	3	7
SW Asia (incl. India and Arab Peninsula, and adj. seas/ocean)	1	4	1	3	9
total:	32	33	30	36	131

CGW (and partial/semi-CGW) detections in **AIRS** data (obvious, strong)					
REGION	2013-2016	2017	2018	2019	total:
Mediterranean region (including all coastal areas)	0	0	0	0	0
Africa (including east Atlantic, west Indian ocean)	3	2	1	2	8
North America and NE Pacific	1	0	0	0	1
South America and SE Pacific	0	1	0	0	1
Australia (and adjacent seas/oceans)	0	0	0	3	3
East Asia (east of India, and adjacent seas/oceans)	2	0	0	0	2
SW Asia (incl. India and Arab Peninsula, and adj. seas/ocean)	1	0	0	1	2
total:	7	3	1	6	17

CGW (and partial/semi-CGW) detections in **AIRS** data (likely present, weak)					
REGION	2013-2016	2017	2018	2019	total:
Mediterranean region (including all coastal areas)	0	0	0	1	1
Africa (including east Atlantic, west Indian ocean)	5	3	1	2	11
North America and NE Pacific	0	1	0	0	1
South America and SE Pacific	0	0	1	0	1
Australia (and adjacent seas/oceans)	0	0	2	0	2
East Asia (east of India, and adjacent seas/oceans)	0	0	0	0	0
SW Asia (incl. India and Arab Peninsula, and adj. seas/ocean)	0	0	0	0	0
total:	5	4	4	3	16

					total:
CGW in AIRS yes (total)	12	7	5	9	33
CGW in AIRS no (total)	16	16	15	24	71
AIRS data not available (total)	4	10	10	3	27

Summary and final remarks

Total of cases with storm-generated CGW in DNB (2013-2019): **131** cases (up to 25 Oct 2019)

- all of these cases also checked for signatures of CGW in AIRS data
- from these, AIRS data available for 104 cases
- from these, only about 30% with some level of GW signatures in AIRS data, related to CGW in DNB

Outcome of this work:

- first global survey of CGW in nightglow (???)
- their link to AIRS data – no obvious correlation between strength of CGW in DNB/nightglow and AIRS (cases of weak CGW in DNB may show strong signatures in AIRS, and vice versa, cases of strong CGW in DNB/nightglow may not show even a trace of corresponding features in AIRS data)
- AIRS band 2043, frequently used for GW observations, may not be the best one for this purpose, other bands (between ~ 2040 to 2060) sometimes show more clear CGW patterns

Future work:

- continuation of this survey (as long as the EOS Worldview continues to provide the night-time DNB imagery, based on any of the NPP or JPSS satellites)
- detailed analysis of selected cases, including Metop IASI data

Data sources, processing and acknowledgements

Satellite data sources (used within this study):

- NASA EOSDIS Worldview – NPP DNB Nighttime global imagery
- Suomi-NPP and NOAA-20 VIIRS data: NOAA CLASS archive
- AQUA AIRS L1B data: NASA EarthData (data coverage here, direct data access here).
- other satellite data and imagery: EUMETSAT

Satellite data processing:

- VIIRS (DNB, I-bands and M-bands) data processed by ENVI software and its VCTK plug-in (by Devin White), final image processing done in Adobe Photoshop.
- AIRS data visualized by ENVI software, additional image processing (selected cases) in Adobe Photoshop.

Support and acknowledgements:

- This work has been partially supported by the CHMI research project „*Dlouhodobá koncepce rozvoje výzkumné organizace (DKRVO) Český hydrometeorologický ústav na období 2018-2022*", financed by the Czech Ministry of Environment.

Additional slides

To be used for the discussion, if needed …

Parallax shift of the airglow features in VIIRS DNB imagery

Parallax shift – apparent displacement of position of an object (feature) at higher altitude with respect to its real location above ground, resulting from a slant view from the satellite.

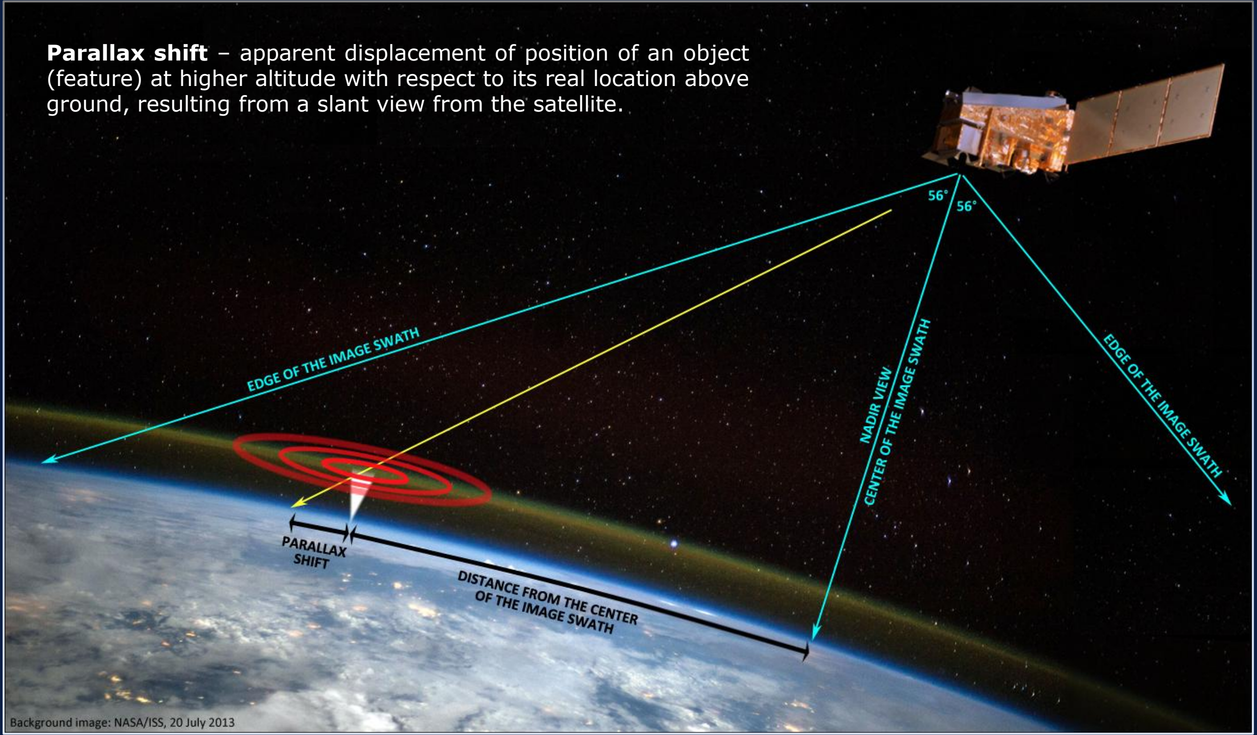

Background image: NASA/ISS, 20 July 2013

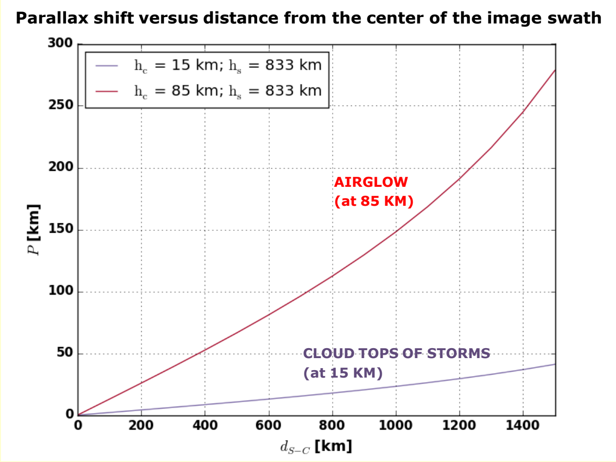

P [km]															
dS-C [km] / hC [km]	100	200	300	400	500	600	700	800	900	1000	1100	1200	1300	1400	1500
15	2.1	4.2	6.3	8.4	10.7	12.9	15.3	17.8	20.4	23.2	26.2	29.4	32.9	36.8	41.0
85	12.9	25.8	39.0	52.5	66.4	80.9	96.1	112.2	129.4	148.1	168.4	190.9	216.2	245.0	278.6

Parallax shift of airglow features in DNB imagery

Values of the parallax shift as related to distance from central line of the satellite data swath, computed for height 85 km and satellite orbit at 833 km.

Parallax shift values for cloud tops of convective storms at 15 km.

Plot above right and table:
Michaela Radová, *michaela.radova@chmi.cz*

Parallax shift of the airglow features in VIIRS DNB imagery – Calbuco Volcano, 23 April 2015

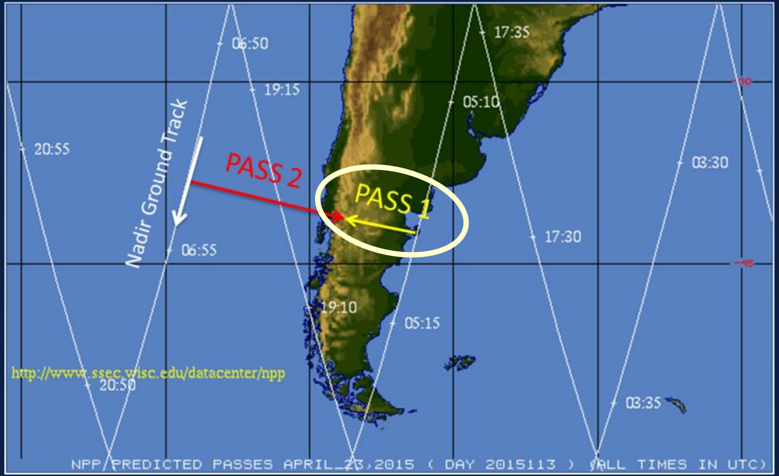

Pass 1 (orbit #18058), 05:12 UTC

The Calbuco volcano region was relatively close to the track (nadir line) of the pass, therefore the parallax shift was rather moderate here.

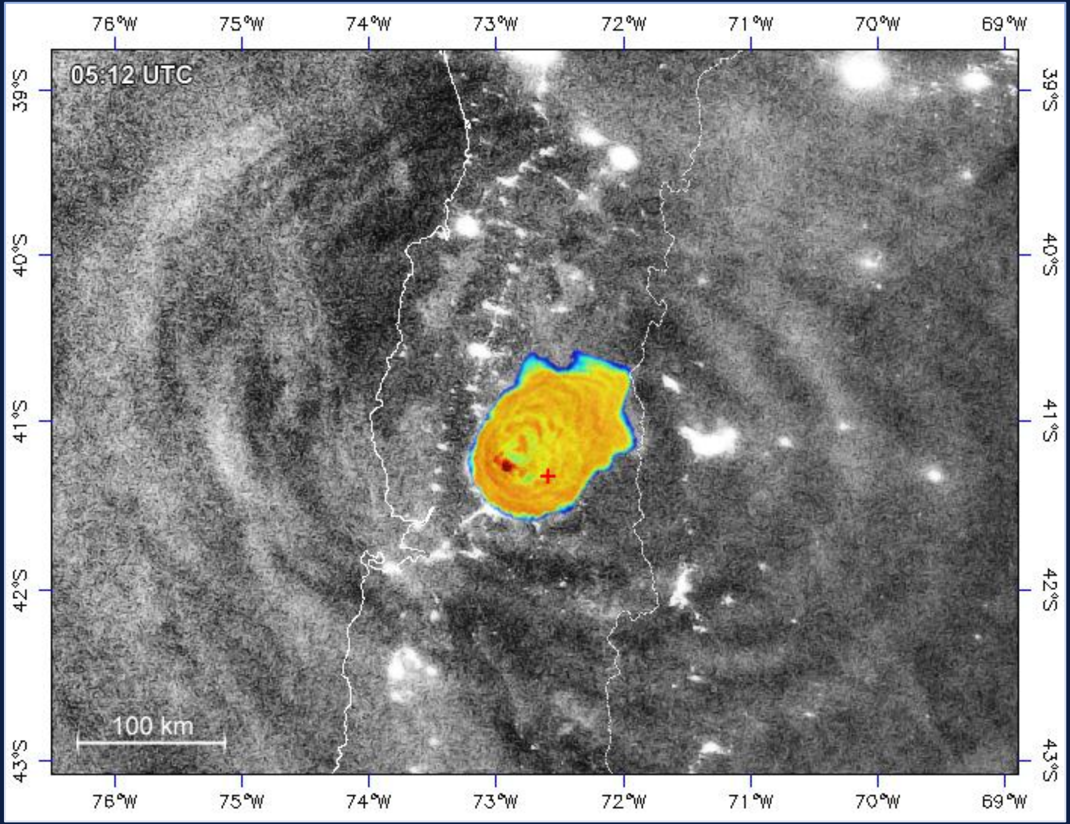

+ – position of the Calbuco Volcano (from IR bands)

Parallax shift of the airglow features in VIIRS DNB imagery – Calbuco Volcano, 23 April 2015

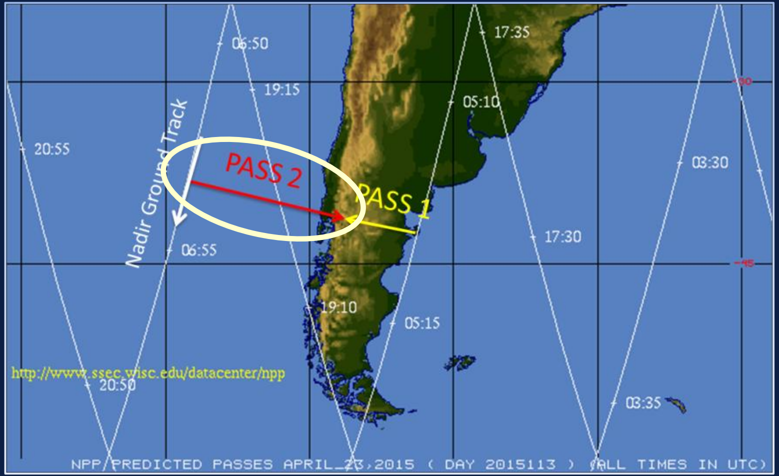

Pass 2 (orbit #18059), 06:53 UTC

For this pass, the Calbuco volcano region was at the very edge of the image swath, therefore the parallax shift is substantial – for the center of the airglow waves about 250 km (in compliance with the calculated values).

Also, given the slant view from the west, the volcano itself can be seen in this pass – both in DNB (light emanated by the lava), and in IR bands (as a hot spot – not shown here).

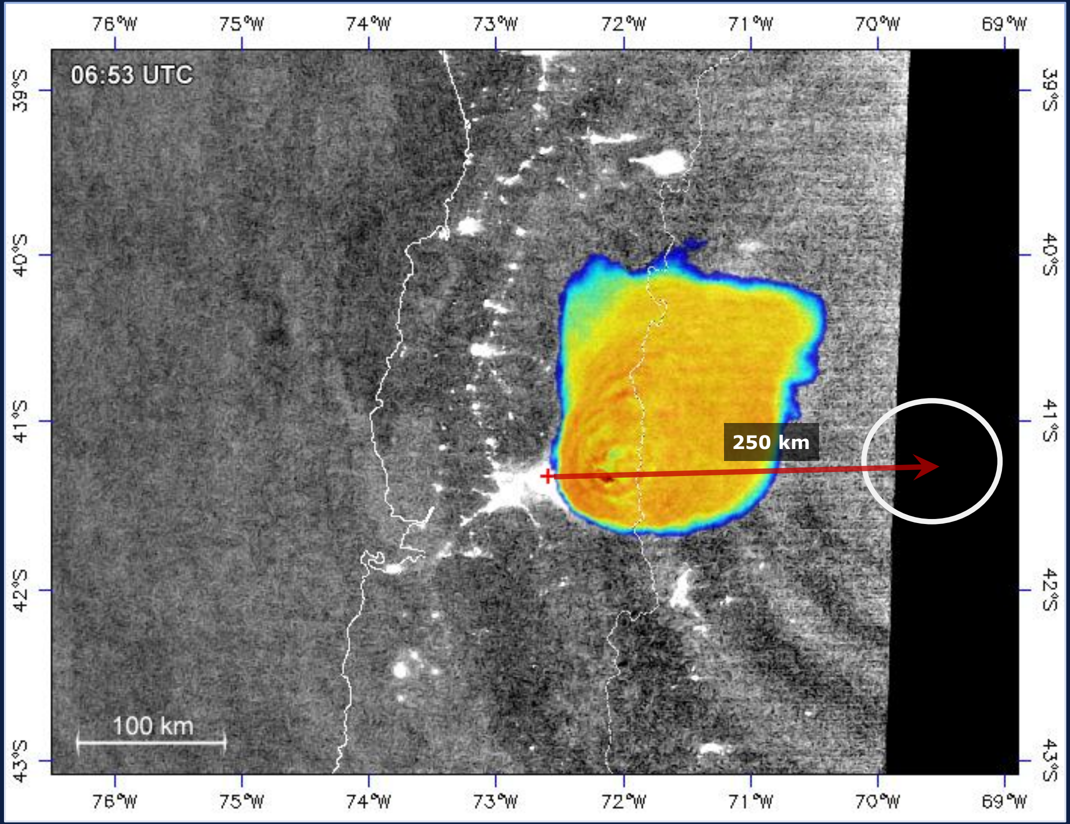

+ – position of the Calbuco Volcano (from IR bands)

Examples of other , non-storm related (gravity) waves in nightglow and DNB observations:

Nightglow in DNB imagery … waves generated by a jet stream, SW Atlantic Ocean, Argentina

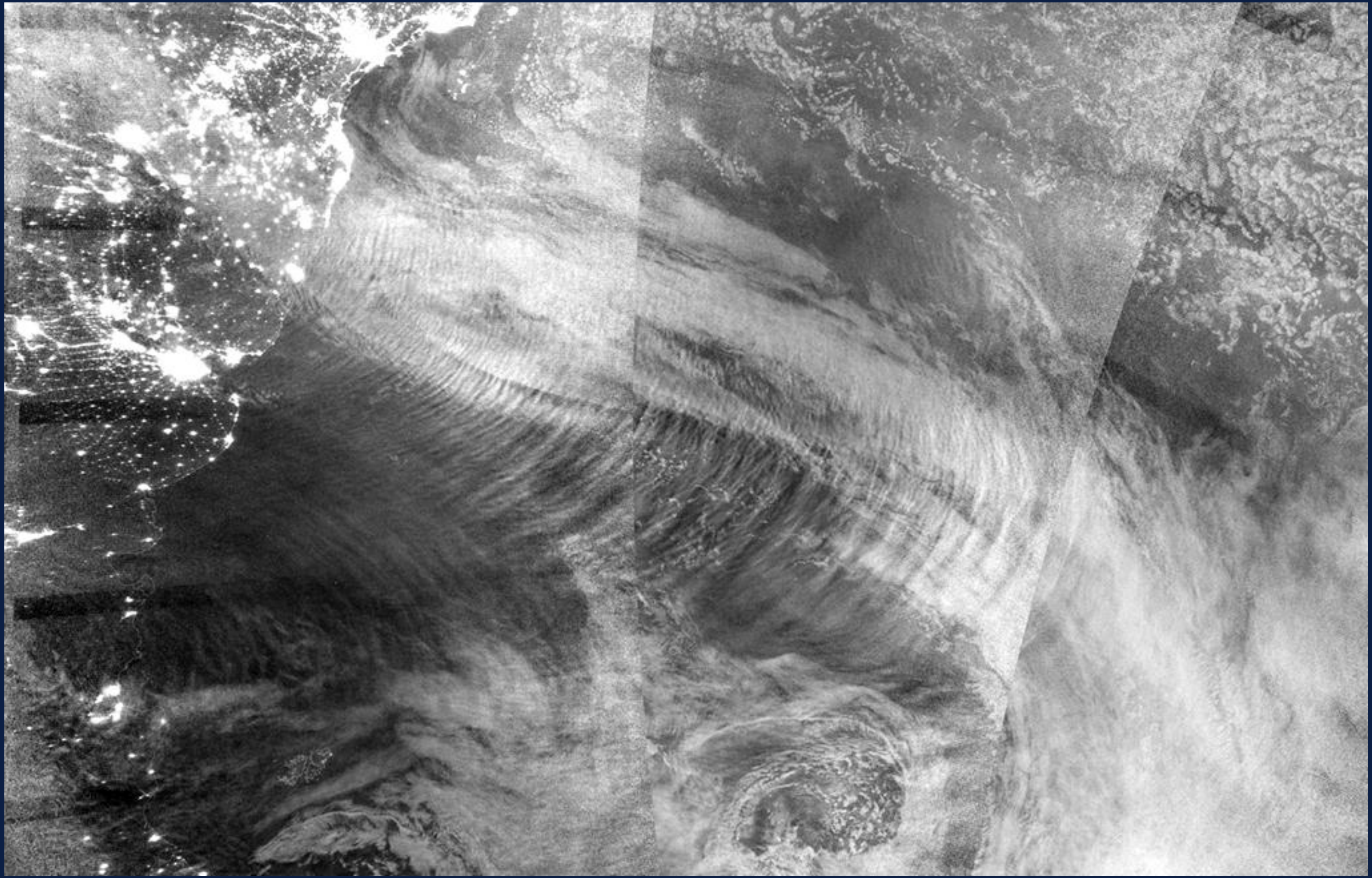

2017-09-16

SNPP, ~ 01 - 04 UTC,
SW Atlantic

Bore waves in nightglow, central Atlantic Ocean

Suomi-NPP, 2017-10-19 02:15 UTC

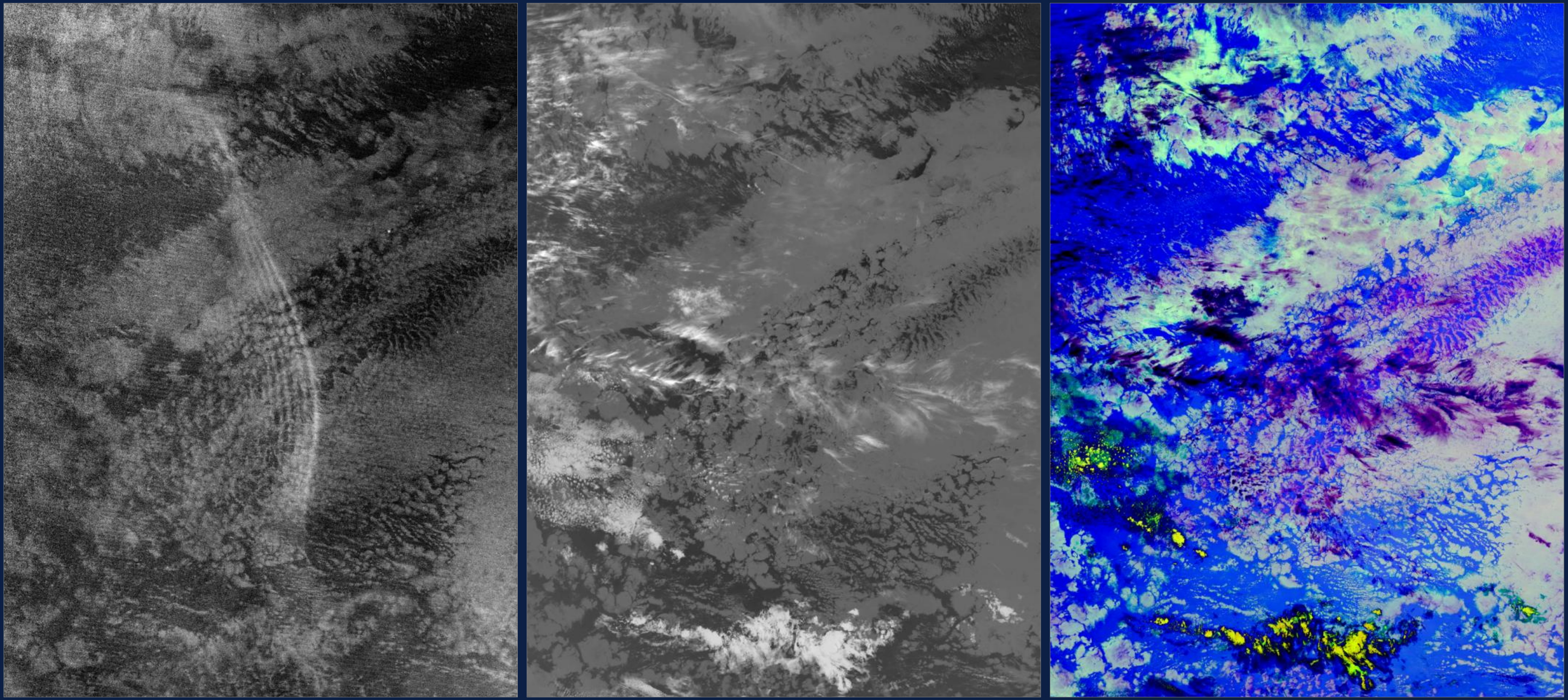

DNB IR M15 RGB Night-M

Concentric gravity waves in nightglow and DNB observations:

north-central and west Africa

Multiple concentric waves in nightglow above western Africa – 11 June 2015

2015-06-11 01:15 UTC

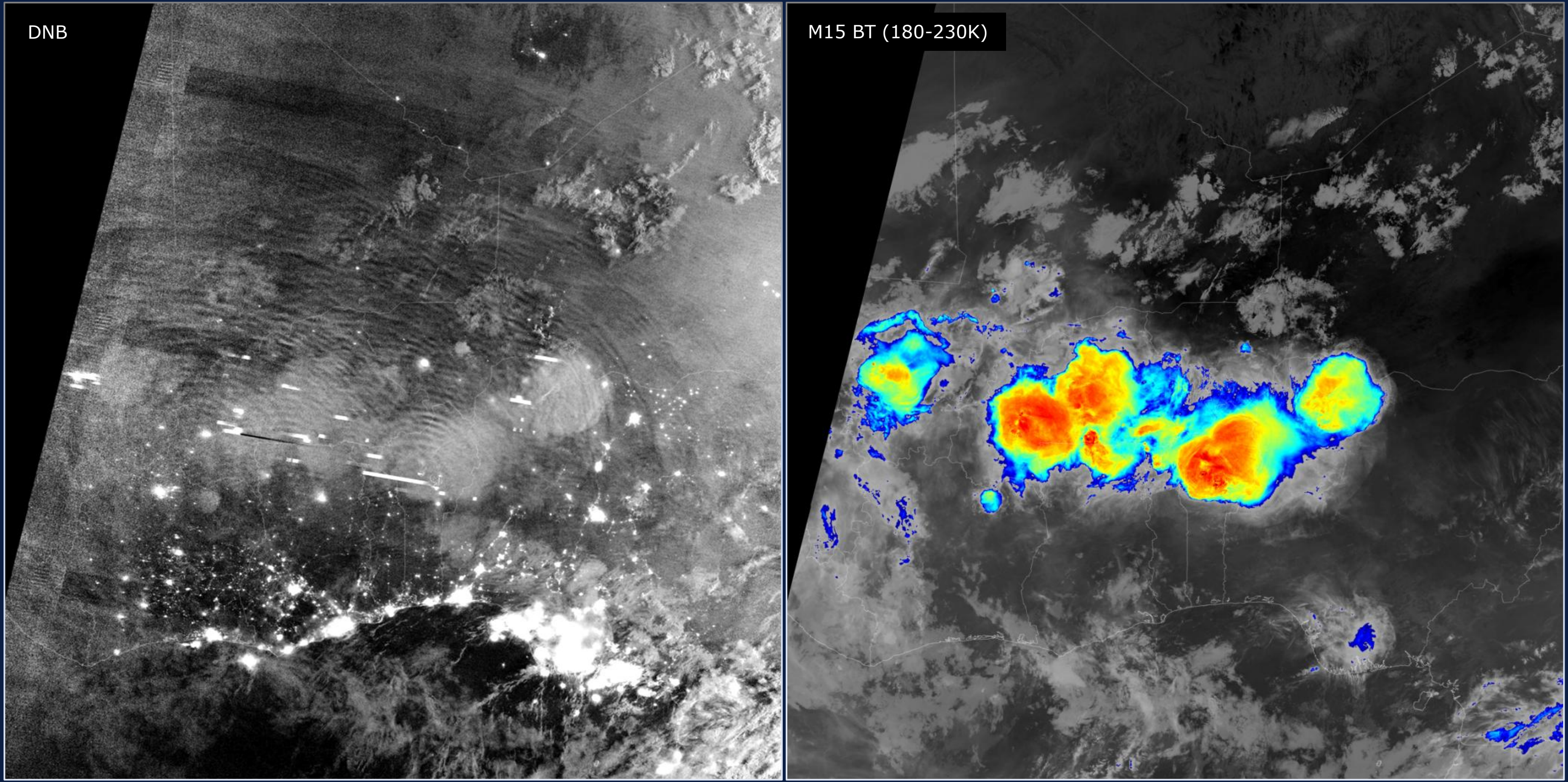

A complex of concentric gravity waves, generated by several storms in the area (several sources of the gravity waves), overlapping each other, spreading mainly north.

Multiple concentric waves in nightglow above western Africa – 11 June 2015

2015-06-11 01:15 UTC

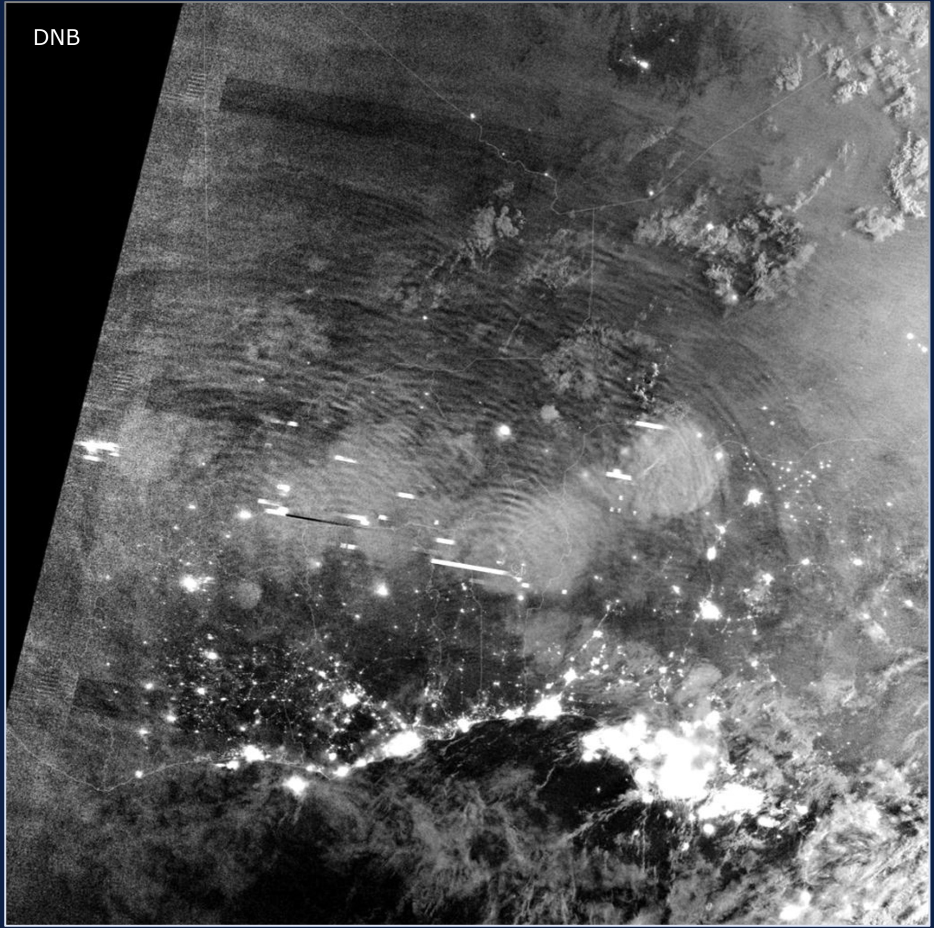

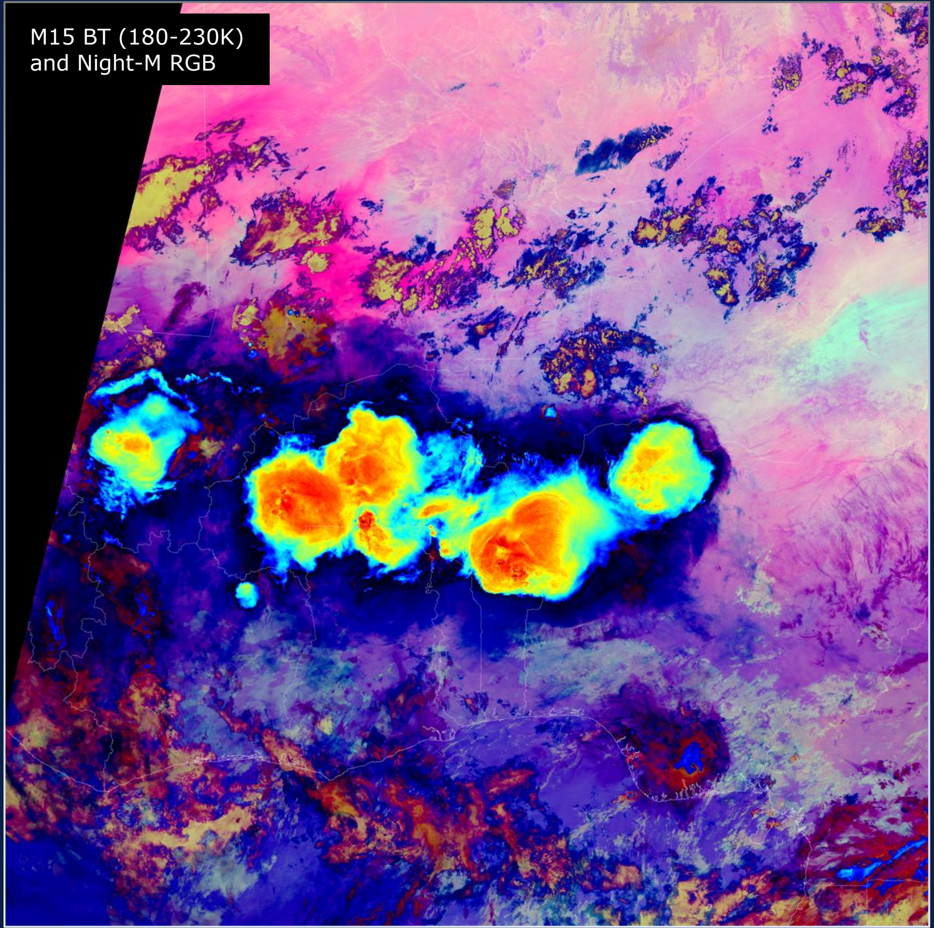

A complex of concentric gravity waves, generated by several storms in the area (several sources of the gravity waves), overlapping each other, spreading mainly north.

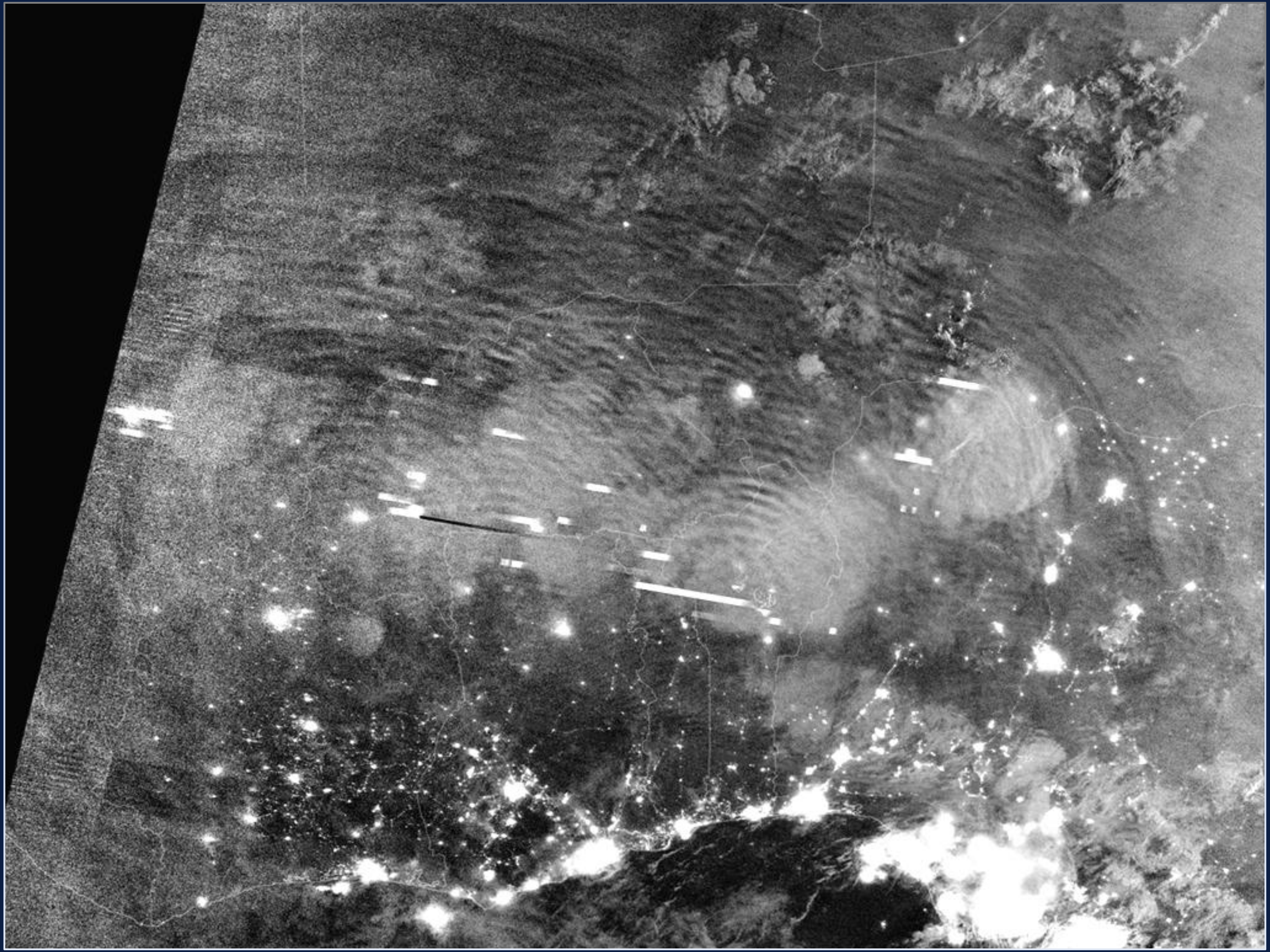

2015-06-11 01:15 UTC

DNB (detail)

Gravity waves in nightglow and DNB observations: northwest Africa

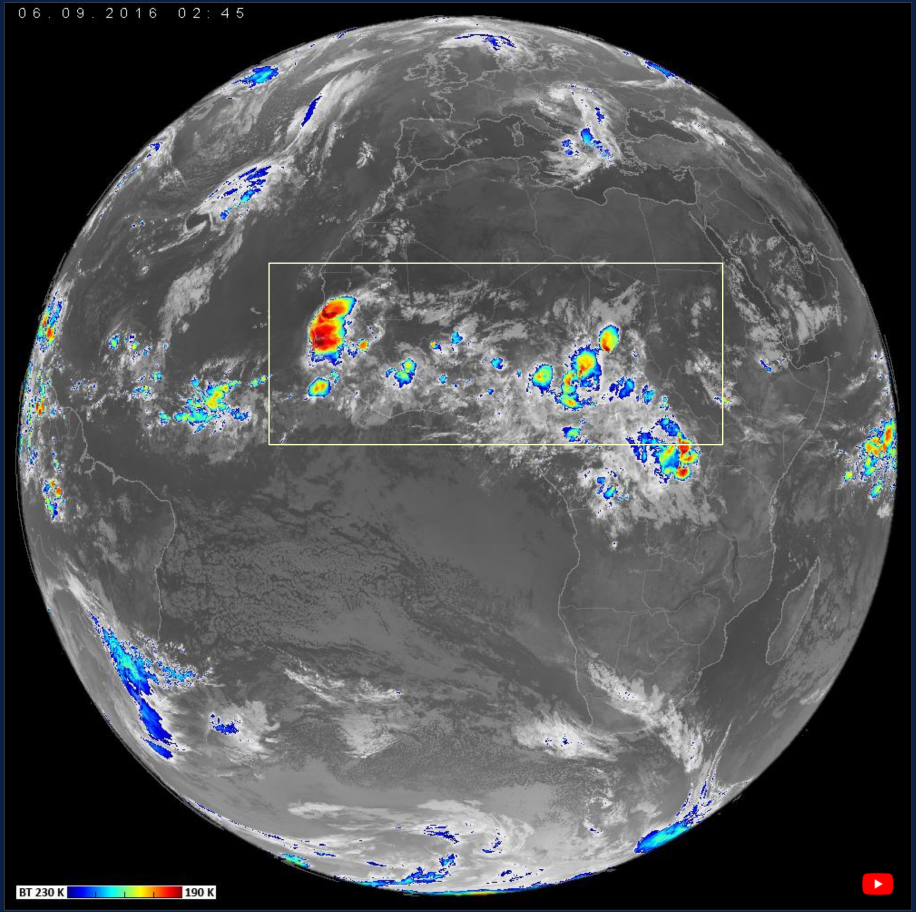

- Area covering south Sahara, Sahel, and north tropics
- strong convective storms forming in easterly waves
- dark background with (almost) no light pollution

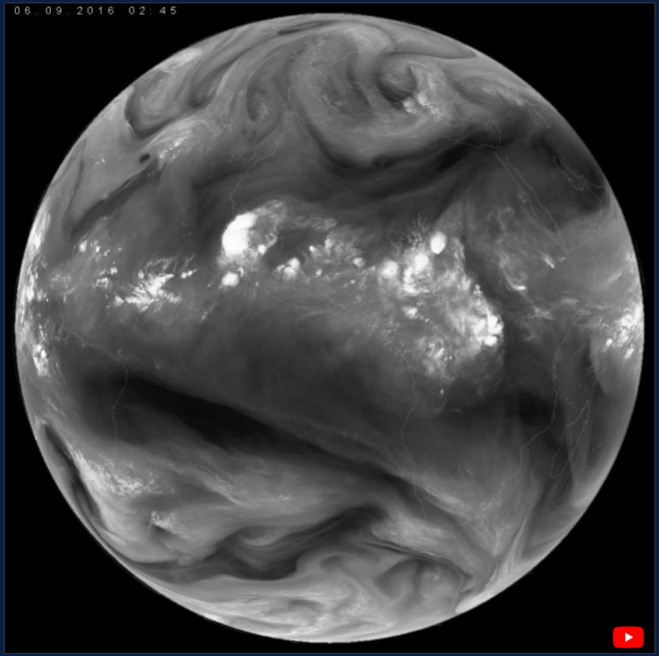

CGW in nightglow above Mauretania and Senegal – 6 September 2016

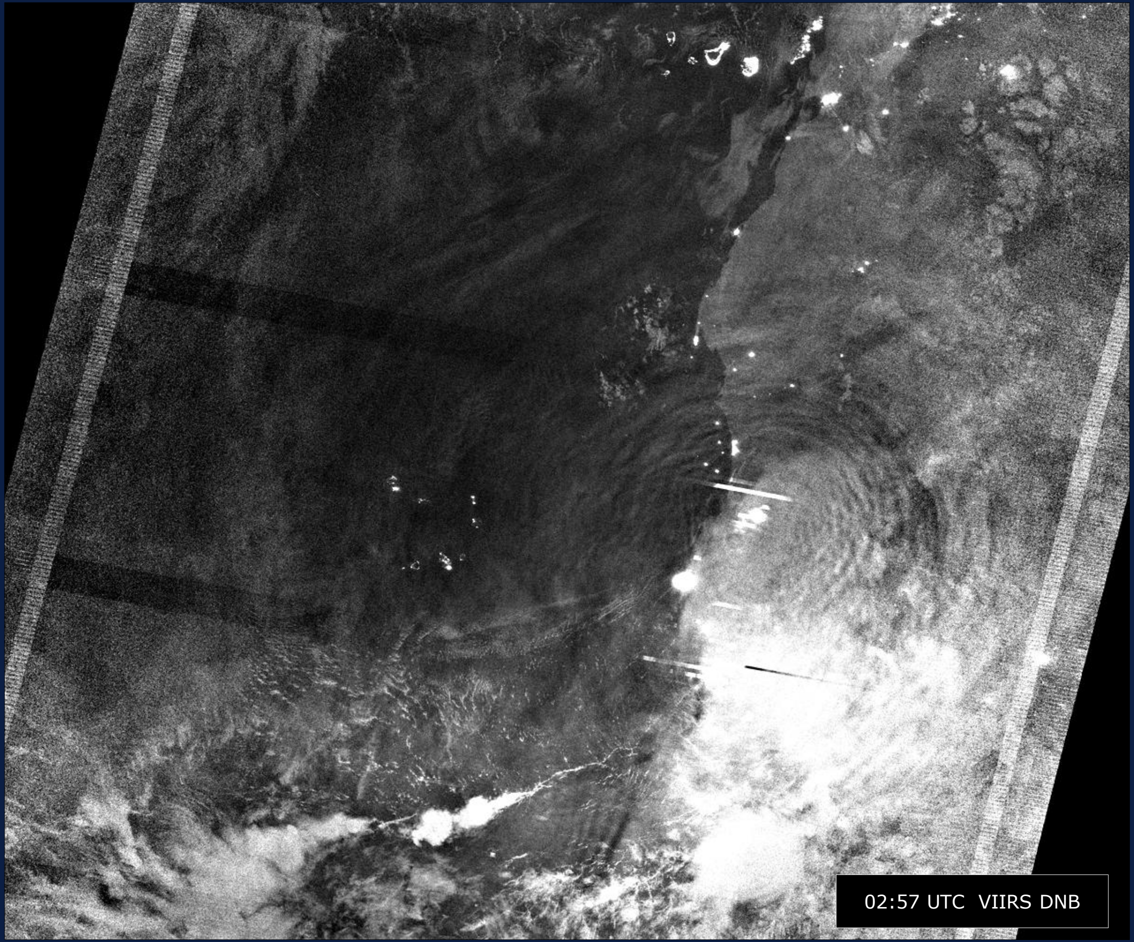

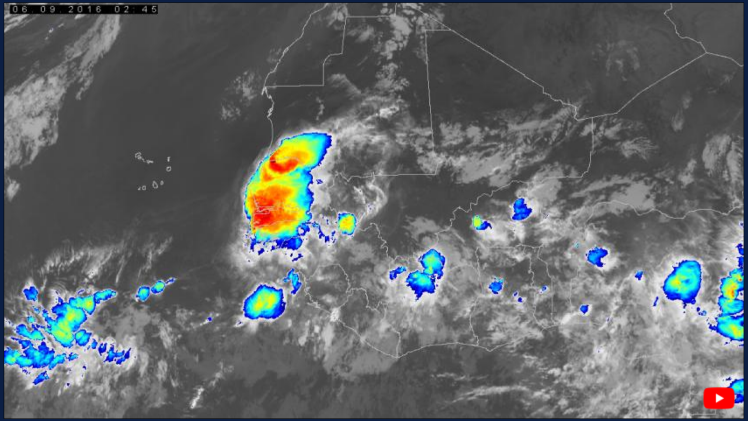

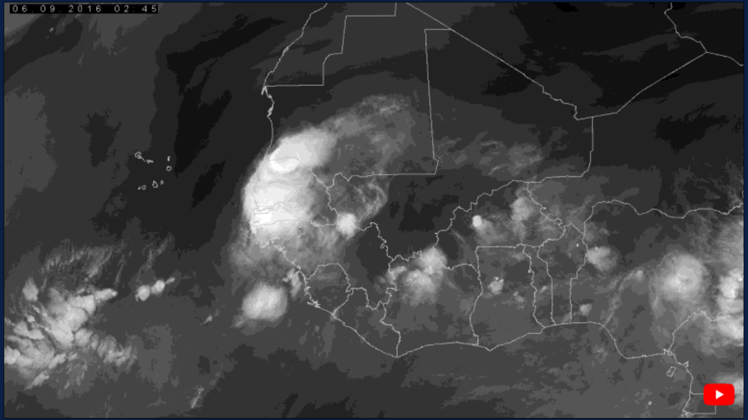

Martin Setvák (CHMI)

CGW in nightglow above Mauretania and Senegal – 6 September 2016

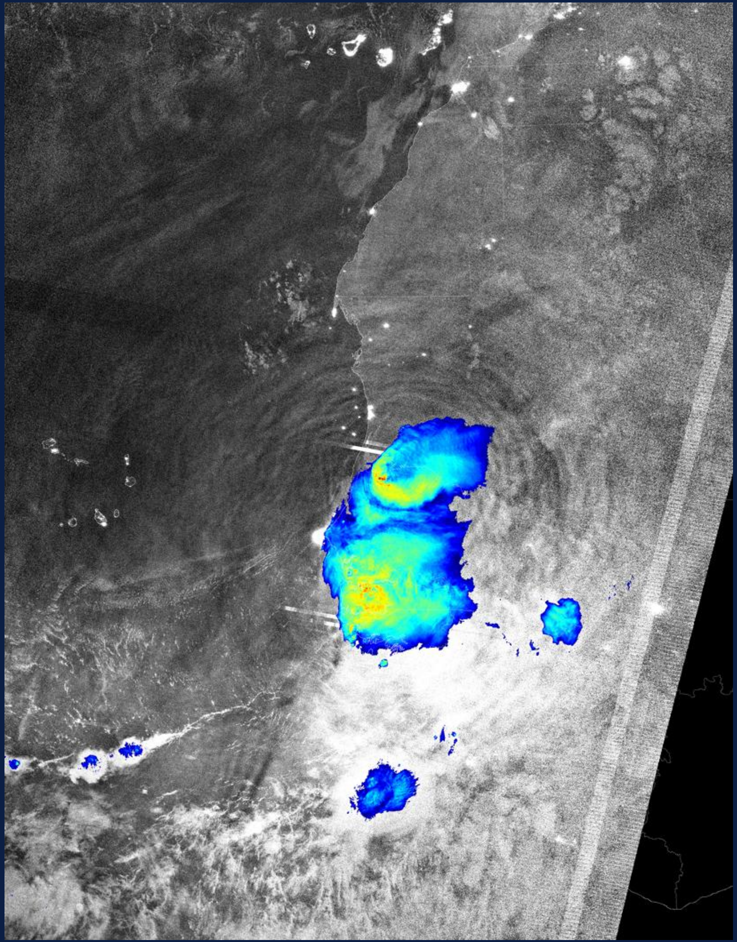

02:57 UTC, VIIRS DNB & band I5 (BT 177-207K)

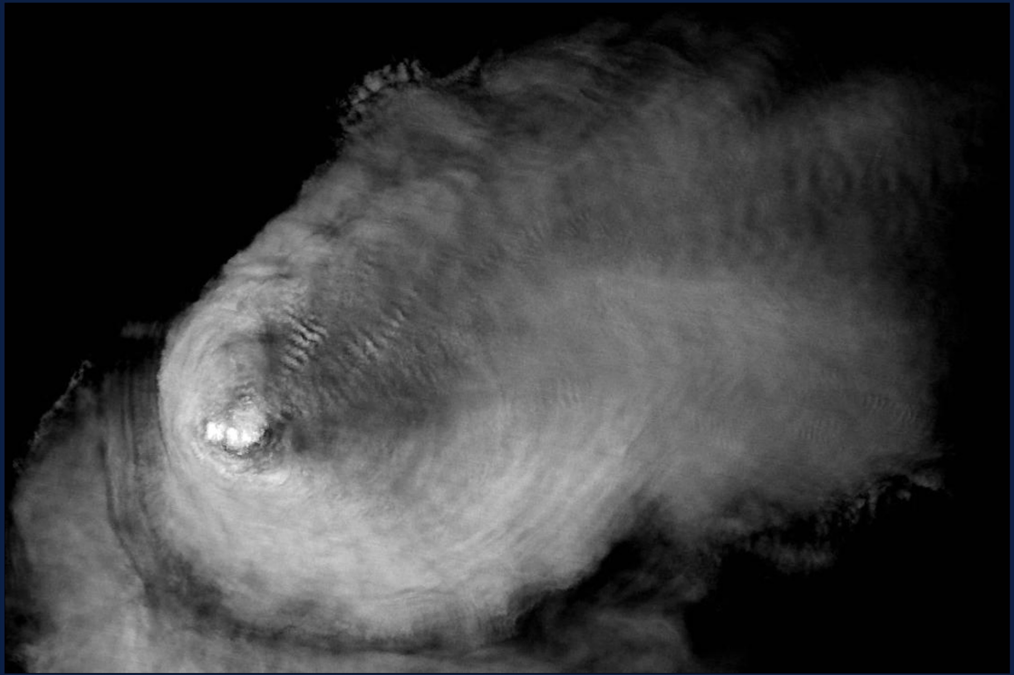

Cloud-top GW, 02:57 UTC, VIIRS band I5 (BT 177-207K, 375m)

CGW in nightglow above Mauretania and Senegal – 6 September 2016

AIRS 02:20-02:30 UTC

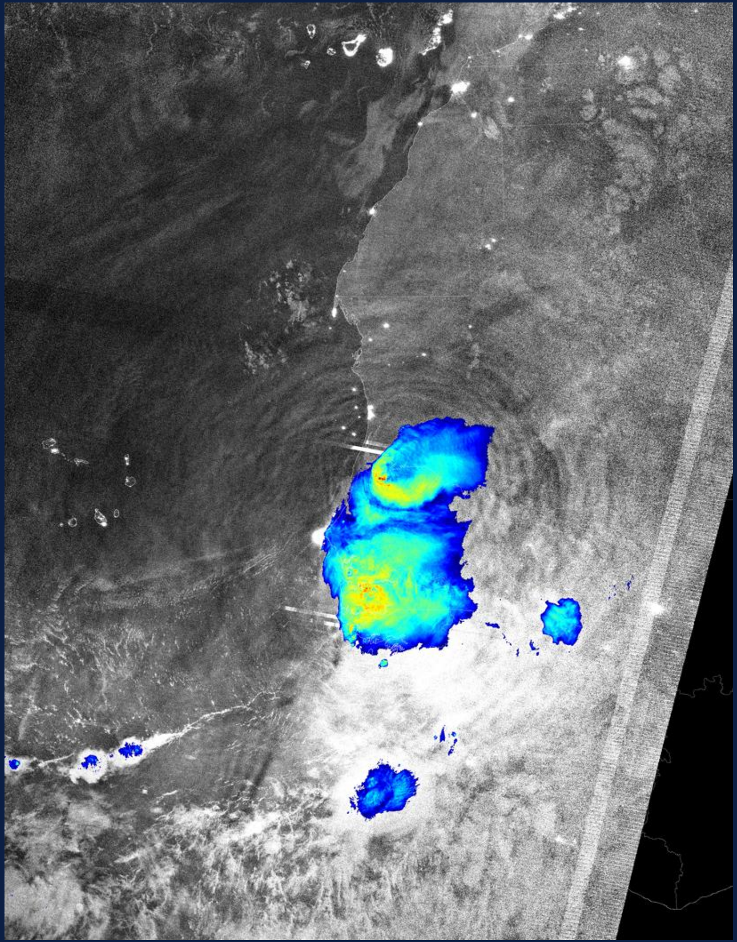

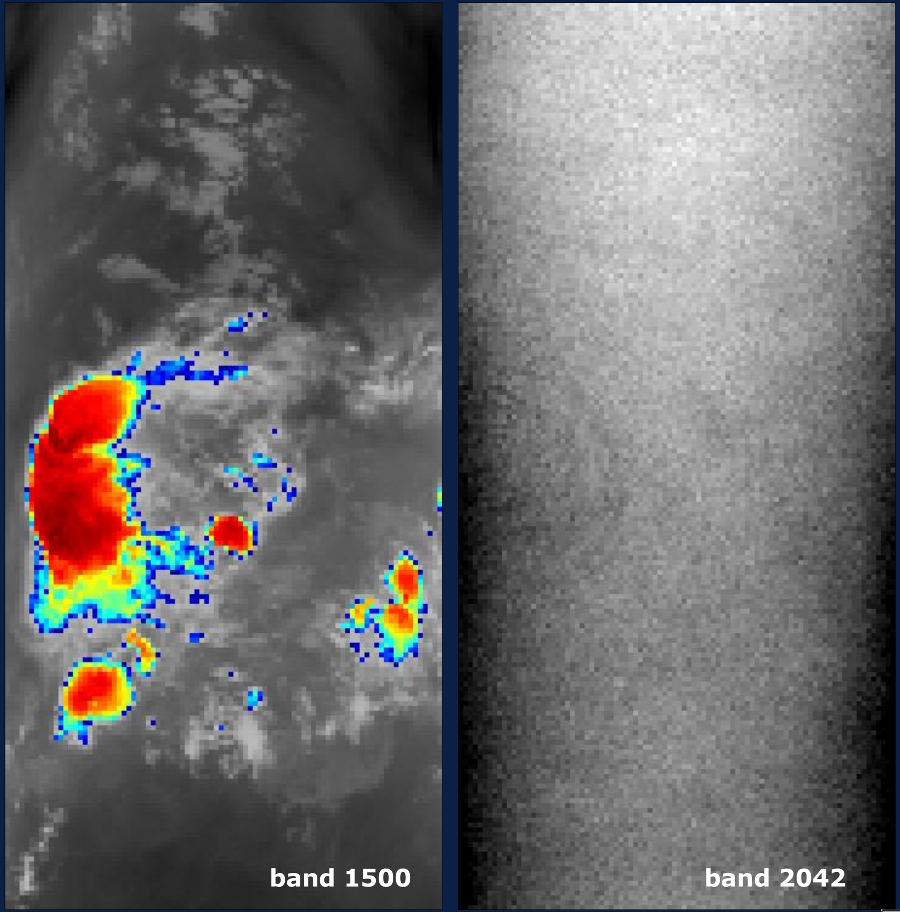

11 April 2014 – gravity waves in nightglow, generated by convective storms east of Taiwan

11 April 2018

16:15 UTC S-NPP
and
17:05 UTC NOAA-20

Range of the waves:
up to about 2500 – 3000 km from their “parrent” storm;

but only within a limited, northeast to southeast sector.

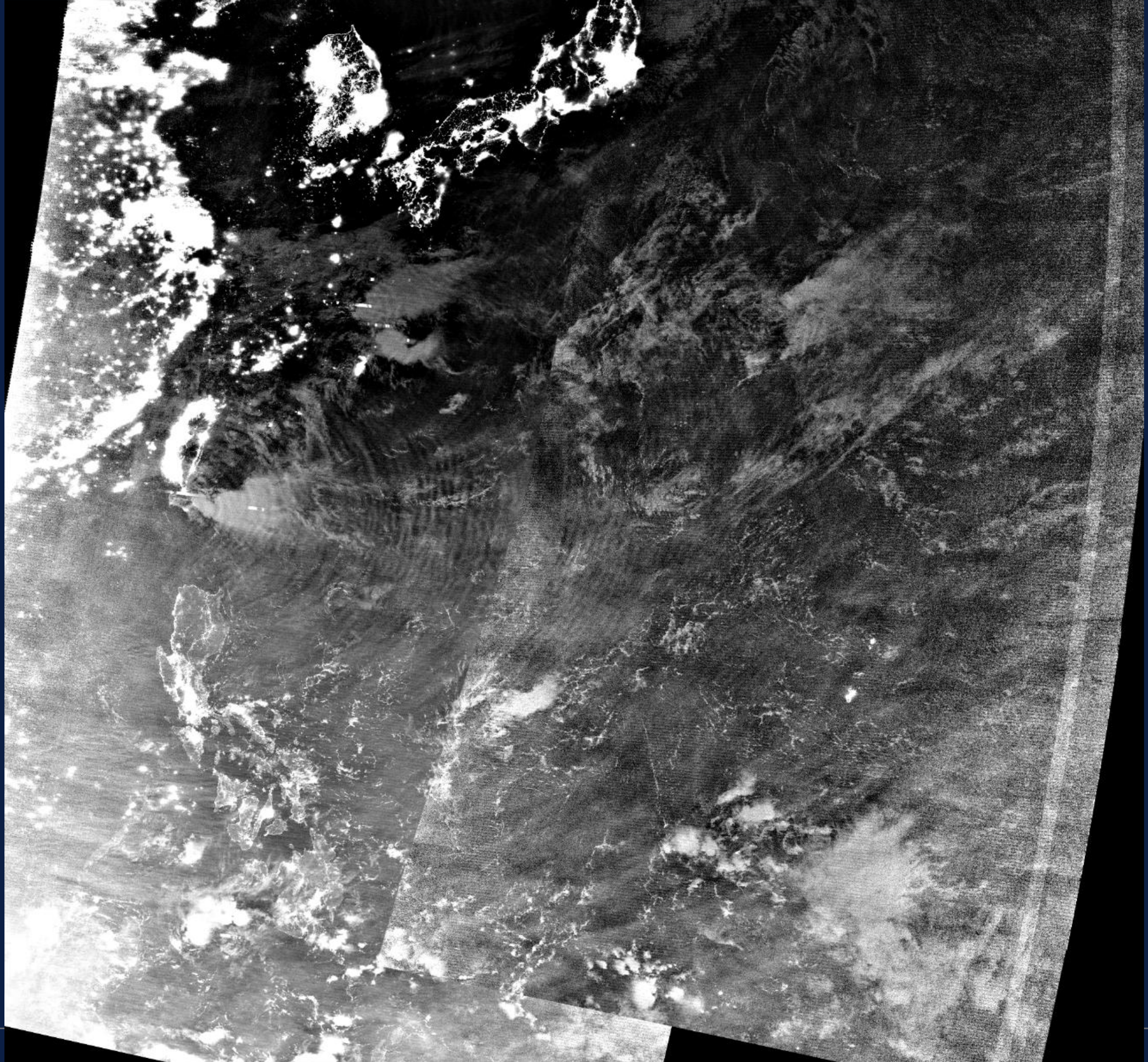

11 April 2018 17:05 UTC – NOAA-20 (JPSS-1)

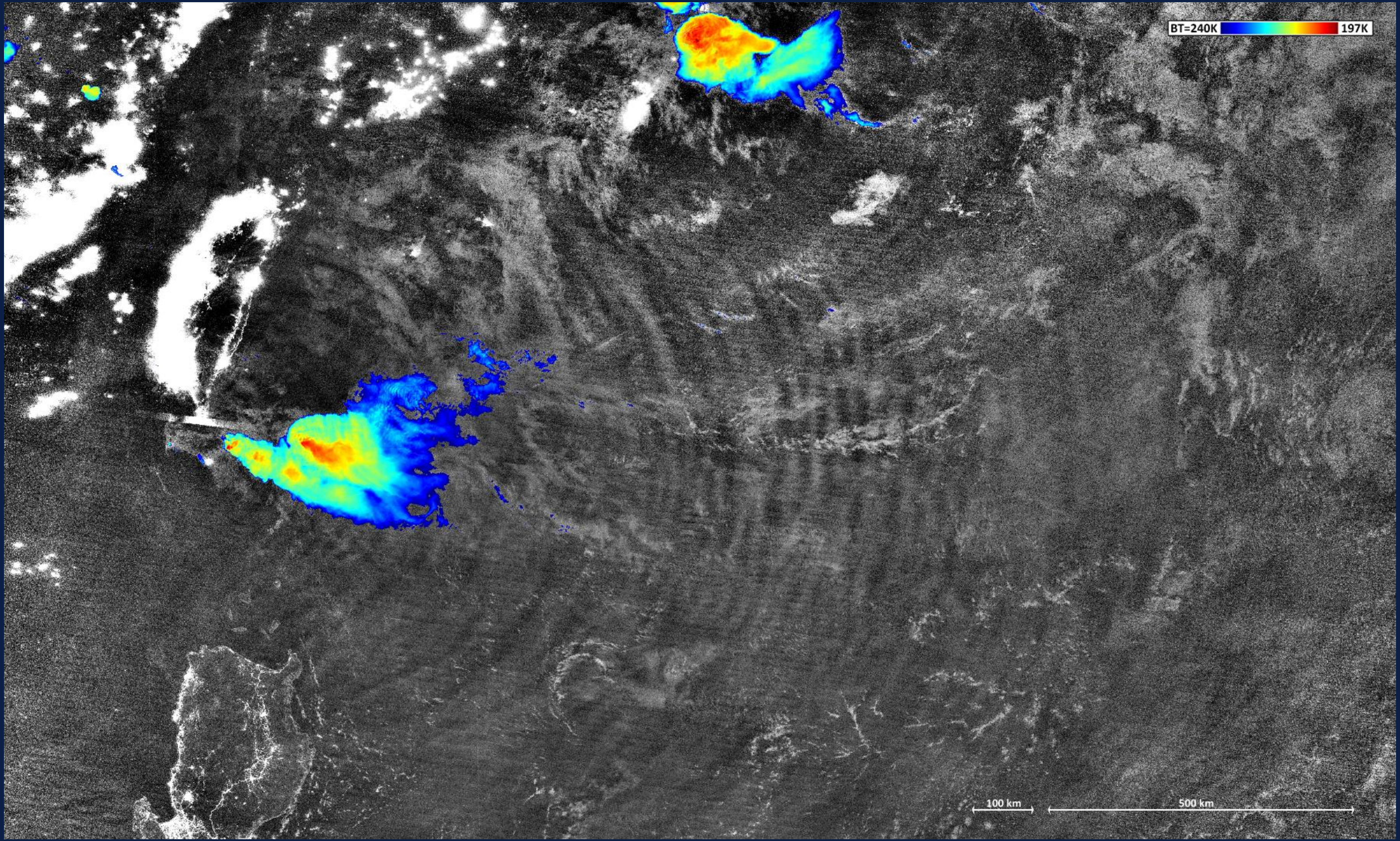

DNB and
IR M15-BT (197-240K)

11 April 2018 17:05 UTC – NOAA-20 (JPSS-1)

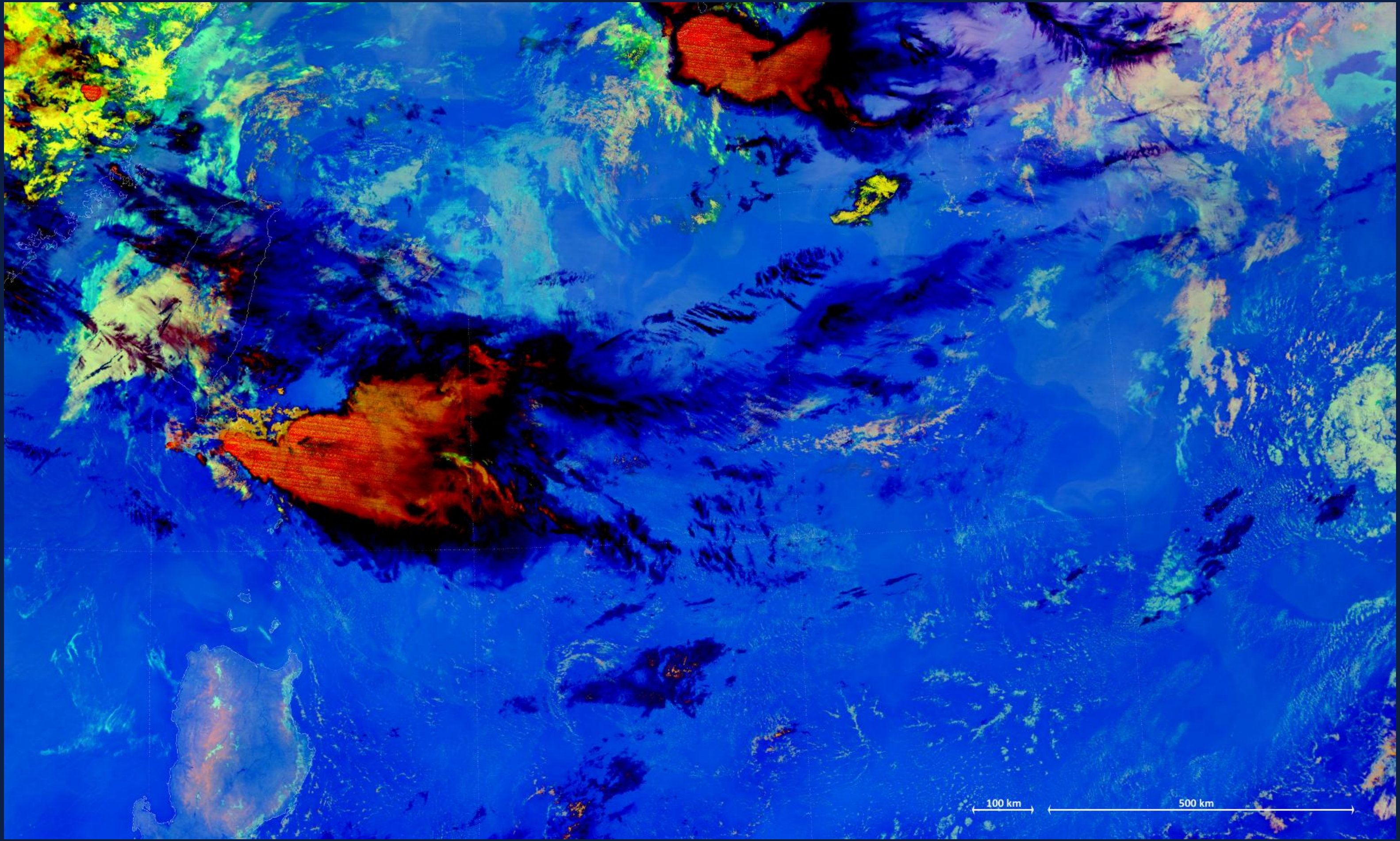

Night microphysics RGB image product

11 April 2018 17:05 UTC – NOAA-20 (JPSS-1)

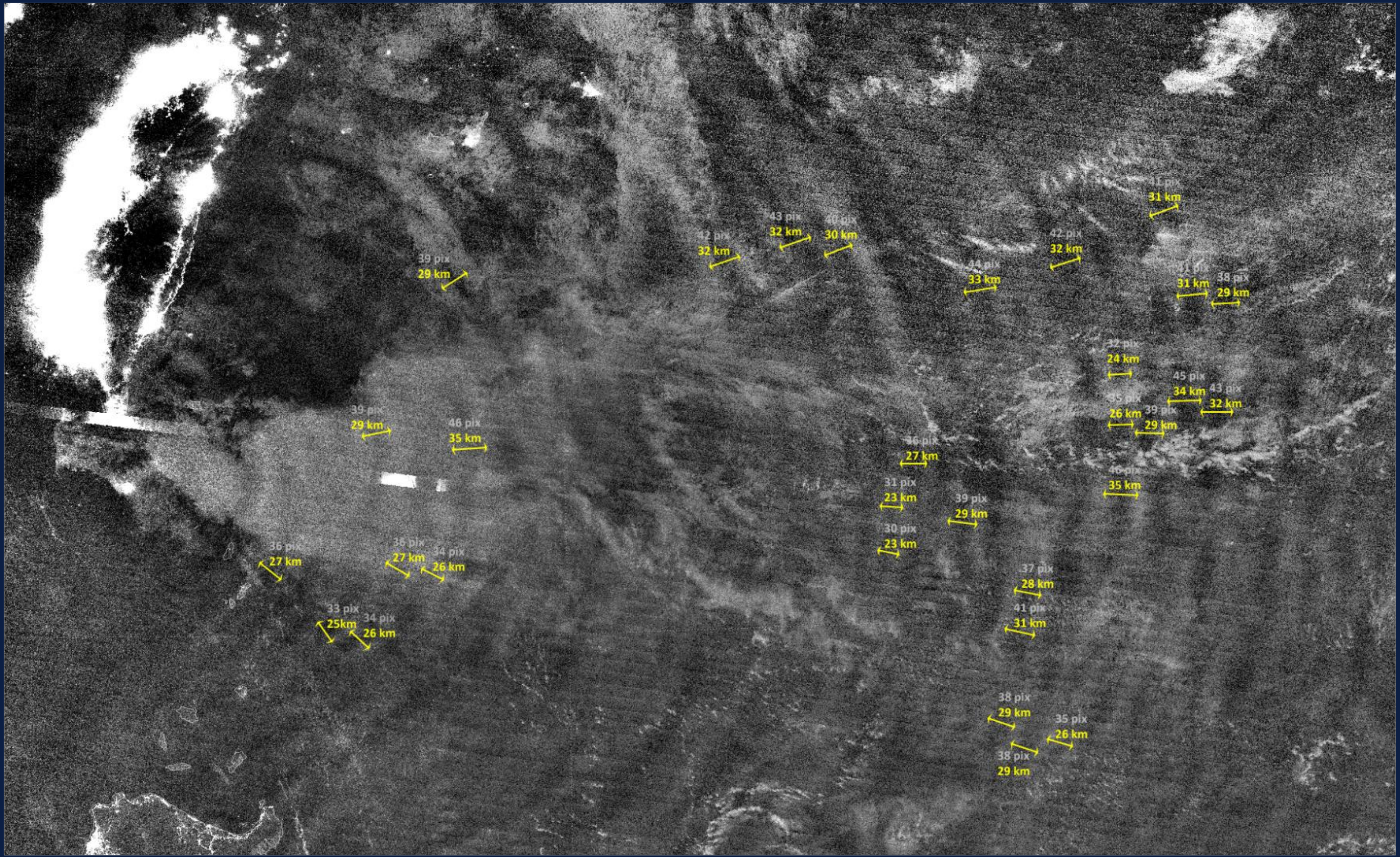

Wavelengths:

about 26 – 32 km